The effect of particle size, temperature and residence time on the yields and reactivity of olive stones from torrefaction

Journal Pre-proof

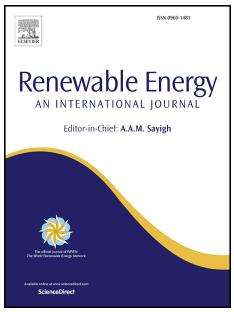

The effect of particle size, temperature and residence time on the yields and reactivity of olive stones from torrefaction

Anna Trubetskaya, Jacek Grams, James J. Leahy, Robert Johnson, Paul Gallagher, Rory F.D. Monaghan, Marzena Kwapinska

PII: S0960-1481(20)31058-2

DOI: https://doi.org/10.1016/j.renene.2020.06.136

Reference: RENE 13813

To appear in: *Renewable Energy*

Received Date: 3 November 2019

Revised Date: 18 April 2020

Accepted Date: 27 June 2020

Please cite this article as: Trubetskaya A, Grams J, Leahy JJ, Johnson R, Gallagher P, Monaghan RFD, Kwapinska M, The effect of particle size, temperature and residence time on the yields and reactivity of olive stones from torrefaction, *Renewable Energy* (2020), doi: https://doi.org/10.1016/j.renene.2020.06.136.

Credit Author Statement: The effect of particle size, temperature and residence time on the yields and reactivity of olive stones from torrefaction

Anna Trubetskaya[a,b,*], Jacek Grams[c], James J. Leahy[a], Robert Johnson[d], Paul Gallagher[e,f], Rory F.D. Monaghan[e,f], Marzena Kwapinska[a]

[a]*Department of Chemical Sciences, University of Limerick, Limerick, Ireland*
[b]*Department of Chemistry, Trinity College Dublin, Dublin, Ireland*
[c]*Institute of General and Ecological Chemistry, Faculty of Chemistry, Lodz University of Technology, ul. Zeromskiego 116, 90-924, Lodz, Poland*
[d]*Arigna Fuels, Arigna Carrick-on-Shannon Co. Roscommon, Ireland*
[e]*School of Engineering and Ryan Institute, National University of Ireland Galway, Galway, Ireland*
[f]*MaREI, the SFI Research Centre for Energy, Climate and Marine, Galway, Ireland*

Anna Trubetskaya: Conceptualization; Data curation; Formal analysis; Funding acquisition; Investigation; Methodology; Project administration; Resources; Software; Supervision; Validation; Visualization; Roles/Writing - original draft; Writing - review & editing

Jacek Grams: Data curation; Formal analysis; Investigation

James J. Leahy: Resources; Writing - review & editing; Funding acquisition; Supervision

Robert Johnson: Writing - review & editing; Project administration; Resources; Supervision; Investigation

Paul Gallagher: Software; Validation; Investigation; Writing of original draft

Marzena Kwapinska: Investigation; Formal analysis; Data curation; Method-

*Corresponding author. anna.trubetskaya@ul.ie

ology; Resources; Writing of original draft; Review & editing

Rory FD Monaghan: Review & editing; Writing of original draft; Funding acquisition; Project administration; Software

The effect of particle size, temperature and residence time on the yields and reactivity of olive stones from torrefaction

Anna Trubetskaya[a,b,*], Jacek Grams[c], James J. Leahy[a], Robert Johnson[d], Paul Gallagher[e,f], Rory F.D. Monaghan[e,f], Marzena Kwapinska[a]

[a]*Department of Chemical Sciences, University of Limerick, Limerick, Ireland*
[b]*Department of Chemistry, Trinity College Dublin, Dublin, Ireland*
[c]*Institute of General and Ecological Chemistry, Faculty of Chemistry, Lodz University of Technology, ul. Zeromskiego 116, 90-924, Lodz, Poland*
[d]*Arigna Fuels, Arigna Carrick-on-Shannon Co. Roscommon, Ireland*
[e]*School of Engineering and Ryan Institute, National University of Ireland Galway, Galway, Ireland*
[f]*MaREI, the SFI Research Centre for Energy, Climate and Marine, Galway, Ireland*

Abstract

Olive stones obtained as a by-product from olive oil extraction in combination with the favourable climate in Mediterranean countries are value-added feedstocks for the energy sector due to low moisture content ($< 20\,\mathrm{wt.\,\%}$), suitable calorific value ($> 18.7\,\mathrm{MJ\ kg^{-1}}$ on as received) and high bulk density (about $750\,\mathrm{kg\ m^{-3}}$). The torrefaction process at Arigna Fuels with high energy efficiency of (above 90 %) improves biomass properties for conversion to a high-value fuel for the use in solid fuel stoves. This study reports the effect of moisture content, organic composition, inorganic matter, particle size, heat treatment temperature and residence time on product yields, O_2/CO_2 reactivity, calorific value, composition and thermal conductivity value of tor-

*Corresponding author. anna.trubetskaya@ul.ie

refied olive stones. Results showed that both lignocellulosic content and ash composition equally influenced the reactivity of torrefied material. For the first time, time-of-flight secondary ion mass spectrometry (ToF-SIMS) showed that the structure of torrefied material from small olive stone particles contains more cellulose than lignin compared to large grains. Importantly from a technological standpoint, the lower heating values of torrefied olive stones ($21.8\,\mathrm{MJ\ kg^{-1}}$) [1] from a small scale reactor were within the range of values for torrefied woodchip briquettes containing high starch binder content which was an increase of $\approx 15\,\%$ when compared to the raw feedstock. The results showed that olive stones of particle size less than 2 mm produced during torrefaction at 270°C for 30 min are the most suitable material and conditions for briquetting due to high solid yield, lower reactivity and low thermal conductivity values. These conditions are recommended for the pilot plant operation using olive stones from the Mediterranean region.

Keywords: torrefaction, slow pyrolysis, olive stones, thermal conductivity, ToF-SIMS

1. Introduction

Increasing human population, global warming, and excessive fossil energy consumption call for the development of sustainable technologies for energy conversion. Bioenergy can be obtained from forestry residues, agriculture wastes, energy crops, manures, and municipal wastes [2, 3]. Regional differences in biomass availability translate into differences in energy practice [4, 5]. The vast and growing amount of agricultural and food waste has become a major concern throughout the world; within the EU, approxi-

mately 700 million tonnes of agricultural wastes are generated annually [6, 7]. The Mediterranean area has significant bioenergy potential from agricultural residues, especially from olive oil production [8, 9]. Olive tree cultivation generates a large amount of biomass from olive tree pruning, which is needed to remove old branches and increase crop productivity [10, 11]. Olive tree pruning biomass, olive leaves and extracted olive pomace have the potential to be used in a biorefinery to produce a range of chemicals through their conversion into fermentable sugars and other valuable molecules [12, 13]. However, only a small amount of olive tree pruning is used as a raw material in power plants due to the feedstock's low density leading to high transportation and storage costs [14, 15]. Prior to olive oil extraction, stones are removed from the olive fruit, washed to provide skin and pith for animal feed and later dried in large piles, as shown in the supplemental material (Figure S-6) [16, 17]. After destoning of olive fruits, the olive pulp is processed using three phase extraction leading to moisture content in olive stones of less than 50 % [18, 19]. The three phase process generates olive stones that are rich in lignin and cellulose compared to the olive cake from the two phase process that has a moisture content greater than 55 % [20]. Since the three phase process generates olive stones with a small amount of oil ranging from 4.5 to 9 %, olive stones are preferred for conversion to high-density briquettes [21]. A combination of destoning, washing and drying, use of removed skin and pith for food purposes, and torrefaction of olive stones and further briquetting might be a potential solution to solid waste problems in this sector worldwide.

Torrefaction is a mild pyrolysis process that converts biomass into a higher carbon material with increased energy density and decreased oxygen

content. Torrefaction contributes concurrently to dehydration, deoxygenation, partial degassing, and structural changes through breaking hemicellulose, lignin and cellulose chains at elevated temperatures. This leads to increased calorific value that improves biomass physiochemical properties during co-firing with coal [22, 23]. One way to improve torrefied biomass handling and combustion properties is by densification into briquettes. Briquettes made from torrefied biomass have many advantages over torrefied feedstocks including reduction of dust, improved handling properties and higher bulk density (up to 66 % greater) [24]. This decreases the cost of shipment and storage [25]. Properties of the original feedstock such as moisture content, heating value, thermal conductivity, ash content, and particle size, affect the quality and yields of torrefied material. As torrefaction involves adding heat to the feedstock, the bulk thermal conductivity of the material needs to be verified to optimise the process. The effect of moisture and particle size on the bulk thermal conductivity of feedstock is of importance as olive stones from different regions have different moisture contents. Thermal conductivity of a bulk material can typically be determined by either transient or steady state methods [26], with apparatus generally calibrated using a bulk material with known thermal conductivity such as sand or gravel. Torrefaction temperatures from 250 to 300°C are used to prevent excessive mass losses from volatile components. The catalytic effect of alkali metal ions is pronounced at temperatures greater than 300°C [27]. Previous studies reported that nearly all the inorganic components remained in the torrefied material without further catalytic effect from alkali metals that could increase the reactivity of torrefied biomass [28]. Hemicellulose starts

degrading between 200 and 380°C, with xylan being the most thermally unstable polymer, followed by glucomannan, as reported by Werner et al. [29]. Thermal degradation of lignin starts approximately at 200°C and finishes at 750°C [30], and the range of thermal devolatilization of cellulose is between 230 and 400°C [31]. As a result, temperature and residence time are the key parameters that have an influence on the degree of torrefaction [32]. In order to achieve a higher yield of torrefied biomass, the particle size of the original feedstock and residence time in a torrefaction unit are the key factors to understand. Both organic content and ash composition are known to affect the yields and physicochemical properties of products from torrefaction [27, 33]. The amount of hemicellulose in original feedstock was suggested to have a greater impact on all gas yields during 200-300°C torrefaction and CO_2 reactivity of torrefied spruce than the fractions of cellulose and lignin [34, 35]. The ash content of wood and herbaceous biomass remain largely unchanged during torrefaction [36, 37]. The most significant changes were observed in the distribution of calcium, magnesium, and manganese, with some change in water soluble potassium [38, 39]. These changes were related to the destruction of carboxylic acid groups and decrease in the concentration of both chloride and sulphur [33]. Small changes in the ash composition during torrefaction have less affect on the O_2 or CO_2 reactivity of torrefied biomass during the thermogravimetric analysis than the differences in lignocellulosic composition of feedstocks [40, 41]. In addition, the increase in torrefaction time from 15 to 120 min leads to a decrease in volatiles and increase in ash content at temperatures greater than 270°C [42]. The size of feedstock particle has a strong effect on the product yield [43, 44]. Larger biomass particles

exhibit a higher conduction resistance and thus a lower heat flux, leading to greater solid char yields during torrefaction [45, 46]. Operating parameters (280°C, for 30 min) have been suggested as the optimum conditions for the torrefaction of olive stones, however, little is known about the influence of residence time and temperature on the yields and composition of torrefied olive stones [1, 47]. Most studies related to biomass pyrolysis have been focused on changes occurring in the bulk of the material [48–50]. However, the modification of the surface layer of torrefied biomass can significantly affect the product yields and thus, further use in combustion and gasification processes [51]. The composition of bulk material is typically characterized using Fourier transform infrared spectroscopy (FTIR), whereas time-of-flight secondary ion mass spectrometry (ToF-SIMS) is used for the characterization of surface properties of single biomass particles. FTIR determines composition by identifying specific functional groups in the chemical structure [50]. ToF-SIMS is used for identification of biomass surface composition through the bombardment of the sample by short pulses of primary ions interacting with the investigated surface [52, 53]. ToF-SIMS has been used to investigate a wide array of solid materials, such as polymers, biological samples, metals, catalysts and archeological objects [52, 54–58]. During ToF-SIMS analysis, chemical bonds are broken with secondary ions initially emitted from the sample and directed to the mass analyzer [59]. In this way molecular level information about the uppermost layer of the analyzed feedstock is obtained with high sensitivity [57]. Limitations of the ToF-SIMS analysis method are mainly related to matrix effects, fragmentation and recombination reactions [60].

The purpose of the present study was to investigate the potential of torrefaction as a conversion technology for the production of bio-fuel with improved properties from olive stones. Laboratory-scale torrefaction experiments were carried out to optimise the Arigna Fuel pilot-scale process. Initial investigations were focused on the potential of gas and char yields from torrefaction of olive stones. In this study, the impact of heat treatment temperature, residence time and particle size on the yields and composition of torrefied olive stones were investigated. This was a starting point for the optimization and redesign of the Arigna Fuel pilot plant into a highly energy efficient and cost effective torrefaction process. The specific objectives of this study were to: (1) relate the product yields from torrefaction with the composition of solid char and gas, (2) understand the influence of heat treatment temperature, particle size and residence time on the physicochemical properties of product yields and (3) develop structure-property relationships governing the CO_2 reactivity of torrefied olive stones.

2. Materials and methods

Olive stones from Tunisia, separated from the degreased spent olives extraction using the three phase method were used in this study. The moisture content of olive stones directly after the extraction was about 40-50 %. However, the moisture content was reduced to less than 20 % due to the high summer temperature and long transportation and storage time leading to the natural evaporation of water [61].

Olive stones from Tunisia were chosen as a feedstock based on their high bulk density and abundance. Particle size, bulk density and skeletal

density of original olive stones were 0.8 to 5 mm, 0.6 g cm^{-3} and 1.5 g cm^{-3} respectively. Olive stones with moisture content of less than 20 % were milled in a laboratory-scale pulverizing mill LM1-P (LABTECHNICS, Australia) and sieved to 0.18-0.425, 0.425-1 and 2-3 mm particle size fractions at Arigna Fuel. Char samples were produced in a laboratory-scale reactor, which is described below, in the temperature range from 200 to 300°C for 30, 60 and 120 min. The properties of non-treated olive stones and torrefied biomass samples were evaluated using a ToF-SIMS, FTIR, thermogravimetric and thermal conductivity apparatus. All of this equipment is described in the following sections.

2.1. Reactor

Torrefaction experiments were performed using a quartz tube reactor, coupled with a condenser cooler and a twin-neck receiving flask where the torrefaction liquids were collected, as shown in Figure 1 and described by Agar et al. [62].

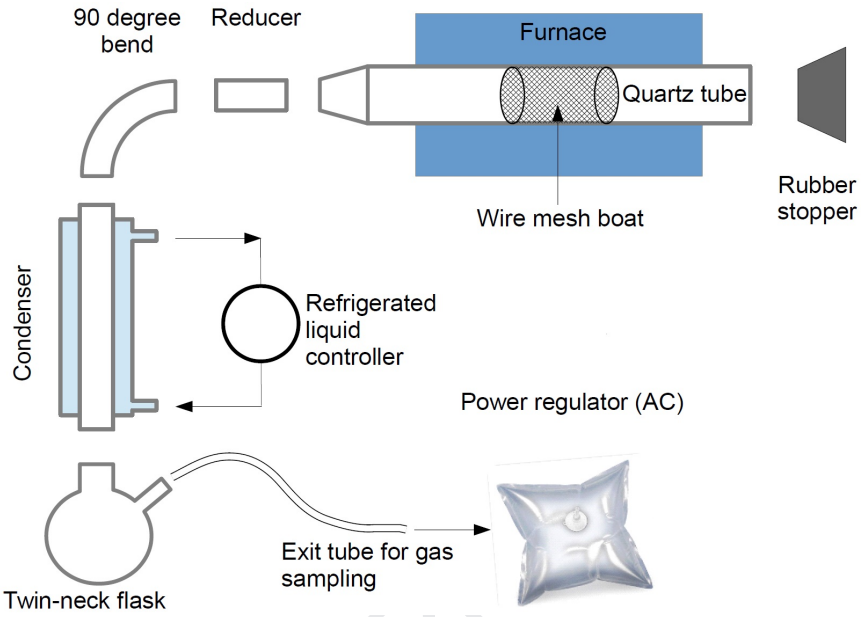

Figure 1: Schematic view of the pyrolyzer at University of Limerick.

The reactor was placed in a horizontal furnace (Carbolite CTF 12/65/550) fitted with a thermal controller (Eurothermal 2416). One end of the reactor tube was open and sealable with a removable rubber stopper. The other end of the cylinder tapered to a ground glass fitting to match a reducer fitting. A 90° bend then followed, leading to the condenser section whose outer jacket was cooled via circulation of a refrigerated liquid maintained at a temperature of -5°C. A twin neck round-bottom flask was connected below the condenser to hold torrefaction liquids. A rubber tube was connected to the other neck of the flask above the liquid level. The other end of this tube was open to atmosphere and fitted with a plastic connector, suitable for attaching gas sampling bags. Milled olive stones were loaded into a cylindrical stainless steel 0.1 mm mesh basket with a length of about 250 mm. The

relative distribution of torrefaction products was determined by the principle of conservation of mass—the combined mass of torrefaction products is equal to that of the initial sample feedstock. The primary assumption is that no liquids exit the apparatus in the vapour phase; all condensable products a represent. Before each torrefaction run, the reactor, the connected glassware, the empty sample basket and the rubber stopper were weighted to within $\pm$ 0.01 g. A sample of feedstock was poured into the basket, and the basket was weighted again. 50 g of milled olive stones were used in each experiment. Circulation of the refrigerated liquid through the condenser was commenced. The furnace was switched on. After approximately 50 min, the reactor reached a steady state and was ready for use (temperature of 200, 250, 270 and 300°C). The sample basket was inserted into the open end of the reactor in one smooth motion and the stopper inserted. After 30, 45, 60 and 120 min, the heating was switched off and the char/torrefied olive stones were cooled to room temperature while still in the reactor. The sample basket and torrefied olive stones were removed from the reactor and weighed. The mass of torrefied olive stones was calculated as the difference between the empty and loaded basket after torrefaction. There were 5 replicate tests carried out for each process conditions. The mass of torrefaction liquid was calculated as the difference in mass of the apparatus (reactor and all components, e.g. the glassware containing condensed and liquid torrefaction products) before and after the series of torrefaction tests. Mass fraction of gas was calculated as the difference between 100 % and the mass of solid char and liquid product.

Gas sampling was done using Tedlar® 0.5 l bags with a polypropylene valve (Restek, Ireland). The bags were clamped to the reactor exit tube

during each torrefaction run. Samples were analysed using a micro gas chromatograph INFICON 3000 (Agilent Technologies, Ireland). The micro gas chromatograph was calibrated using a mixture of H_2, CH_4, N_2, CO, CO_2, C_2H_2, C_2H_4, C_2H_6, and H_2S. The O_2 content was calibrated using air.

2.2. Characterization of torrefaction products

Karl Fischer titration. Karl Fischer titration was carried out using a KF1000 volumetric titrator (Hach, Germany). Tar samples were first dissolved in anhydrous methanol and then injected into the titration cell. All titrations were carried out at room temperature and the experiments had an error of $\pm$ 0.5 % water content.

Time-of-Flight Secondary Ion Mass Spectrometry. ToF-SIMS measurements were performed using a TOF-SIMS IV instrument (ION-TOF GmbH, Germany) equipped with a 25 kV pulsed Bi_3^+ primary ion gun in the static mode. The samples were pelletized prior to analysis and attached to the sample holder using double-sided tape. For each sample, at least three spectra were collected from different locations. The analyzed area corresponded to a square of size 100 μm x 100 μm. A pulsed electron flood gun was used for charge compensation.

FTIR Spectroscopy. The solid residue was analyzed using a Cary 630 FTIR spectrometer (Agilent, USA). All absorption spectra were obtained in the 4000-600 cm^{-1} range by 100 scans at 4 cm^{-1} resolution. For background, 200 scans were acquired. All samples were measured in triplicate.

Thermogravimetric analysis. The torrefied olive stone samples were firstly crushed to a fine powder in a mortar with a ceramic pestle. Thermal decomposition of torrefied biomass samples was determined using an atmospheric pressure thermogravimetric instrument (Mettler Toledo, USA). The reactivity of solid char in 20 % volume fraction CO_2 (20 cm^3 min^{-1} of CO_2 and 80 cm^3 min^{-1} of N_2 measured at 20°C and 101.3 kPa) was determined by loading 5 mg of sample in an Al_2O_3 crucible. The torrefied olive stone samples were firstly heated up to 110°C and kept for 30 min isothermally for drying. The dried samples were subsequently heated to 1100°C at a constant heating rate of 10 °C min^{-1}. All measurements were conducted in duplicate to establish reproducibility.

Thermal conductivity measurements. A steady state conduction apparatus, as shown in the supplemental material (Figure S-1), was designed to measure the bulk thermal conductivity of the biomass material. The biomass sample was contained within a ceramic flue liner of inner diameter 200 mm and height 200 mm. This was surrounded by insulating earthwool with a thermal conductivity of 0.044 W $m^{-1}K^{-1}$ to reduce heat losses to the environment. This setup was placed on top of an induction heater with a 200-mm diameter induction disc on top of the heated surface. Platinum resistance temperature sensors (Pico Technologies, UK) were located at specific distances from the induction heater and used to measure the temperature gradient in the sample. The PT100 sensors were connected to a data logger which was then connected to a laptop used in conjunction with software available from the supplier. An aluminium frame was placed over the apparatus to which an extractor fan was attached, to remove any volatile gaseous emissions from

the sample under test and to help maintain a constant temperature by inducing forced convection cooling of the metal disc placed on top of the sample container. For each test run, the apparatus was filled with the sample material and the induction heater was set to an appropriate power setting. The temperature readings from the PT100 sensors were displayed using the software on the laptop connected to the data logger. By examining the time profiles for the measured centreline temperature distribution, it was possible to determine when steady state conditions were reached. Once steady state conditions were identified, the PT100 sensors were moved outwards from the sample centerline to the inner wall of the flue liner. The steady state temperature distributions at both the centreline and outer edge of the sample were used as inputs to an in-house two-dimensional steady state finite volume solver created in MATLAB. This model iteratively compared predicted and experimental centreline temperature distributions for a range of thermal conductivity values. The bulk thermal conductivity of the sample was then identified as the value that yielded the minimum error margin between the modelled and measured temperature distribution. Two test runs were carried out for each material and the average of these two runs gave the bulk thermal conductivity for the sample.

3. Results

3.1. Original feedstock characterization

Compositional analysis of olive stones after 6 months of storage at Arigna Fuel pilot plant and further milling and sieving is shown in Table 1. As expected, olive stones consist primarily of carbon and oxygen, with a HHV

similar to other biomass types [63]. The ash content of olive stones was greater than that of olive pulp. However, olive pulp contained more calcium than olive stones [1, 64]. Table 1 showed that the HHV and ash content decreased with the increasing particle size, whereas the ultimate analysis did not show large differences between the olive stones of different particle size.

Table 1: Proximate, ultimate and ash compositional analysis using olive stones milled to 0.18-0.425, 0.425-1 and 2-3 mm.

Properties	**0.18-0.425 mm**	**0.425-1 mm**	**2-3 mm**
	Proximate analysis / DIN EN 14775		
Moisture, (wt. % ar)	15.5	9.8	11.2
Ash at 550°C/815°C, (wt. % db)	0.8	0.6	0.4
Volatiles, (wt. % db)	76	78	75.5
HHV, (MJ kg^{-1} ar) / ISO 1928	20.3	19.7	19.5
LHV, (MJ kg^{-1} ar) / ISO 1928	18.7	18.2	18.0
Ultimate analysis, (wt. %, dry basis) / DIN EN 14775			
C	44.9	46.8	47.2
H	5.8	6.2	6.1
N	0.2	0.3	0.1
O	48.3	46.1	46.2
S	0.03	0.03	0.02
Cl	0.01	0.02	0.02
Ash compositional analysis in feedstock, (mg kg^{-1}, dry basis) / DIN EN 15290, [65]			
Al	40	20	40
Ca	2400	2600	1900
Fe	500	200	40
K	2500	2400	3200
Mg	250	100	80
Na	60	40	70
P	100	60	50
Si	1100	600	350
Ti	3	3	2

Regarding mineral matter composition, content of silica, calcium, iron, phosphorus and magnesium in the ash increased with the decreasing particle size of olive stones.

3.2. Ash compositional analysis

The ash content in the 0.18-0.425 mm particle size fraction increased with torrefaction temperature, whereas the larger particle size fractions did not show any significant change in ash content in the temperature range 200 to 300°C (see Table S-4), confirming previous results [36, 66, 67].

The effect of torrefaction temperature, residence time and particle size on the content of ash forming elements is presented in Figure 2. Torrefied olive stones showed a high concentration of potassium, calcium and silicon along with smaller amounts of sulfur, chlorine, phosphorus, aluminum, iron, sodium, and magnesium. The relative concentration of calcium in the 0.18-0.425 mm particles increased in samples torrefied at temperatures above 250°C compared to original feedstock and olive stones torrefied at lower temperatures, as shown in the supplemental material (Table S-1). In addition, the calcium content in olive stones of particle size greater than 2 mm torrefied at 270°C for 30, 60 and 120 min changed only slightly. In literature, there are contradicting conclusions about the effect of alkali metals on yields of solid product from torrefaction. Saleh et al. [68] reported that an increasing alkali metal content decreased solid product yield at 270 and 300°C (6 different biomasses), whereas González Martínez et al. [27] reported that alkali metals did not show any influence on the extent of solid degradation during torrefaction for 16 various biomasses.

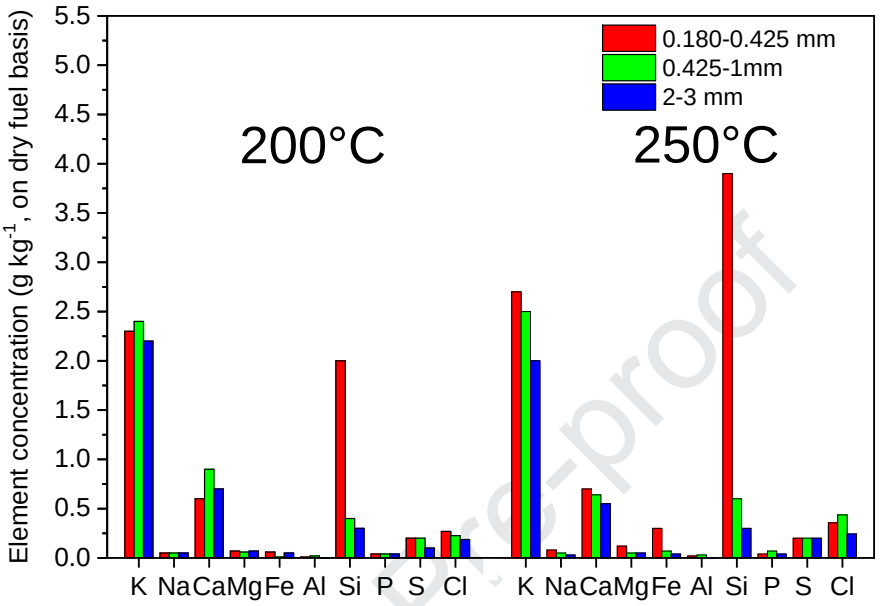

2(a):Torrefied olive stones reacted at 200 and 250°C

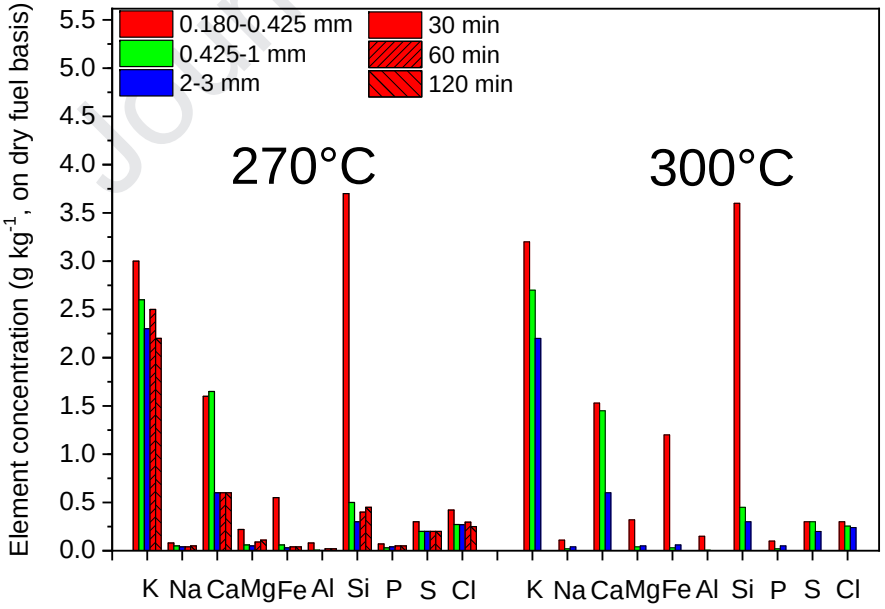

2(b):Torrefied olive stones reacted at 270 and 300°C

Figure 2: Ash compositional analysis of torrefied olive stone particles sieved to 0.18-0.425, 0.425-1 and 2-3 mm size fractions at 200, 250, 270 and 300°C reacted for 30, 60 and 120 min.

The results from the current study show that yields of the solid char at the torrefaction temperatures of 270 and 300°C were strongly influenced by the presence of calcium in the original feedstock and less by potassium (Figure 3). The increased amount of $CaCO_3$ in olive stones could lead to the destruction of the crystalline cellulose structure in olive stones, leading to the decrease in solid char yield during torrefaction [1, 69–71].

The concentration of silicon and iron remained the highest in the smallest fraction of the olive stones and it increased with torrefaction temperature. The concentration of calcium was mainly affected by process temperature and it increased with temperature. The differences between the particle size fractions with respect to silicon, potassium and calcium especially at higher temperatures were large, indicating the influence of particle size on the content of ash forming elements after torrefaction.

3.3. Product yields

Product yields from torrefaction of olive stones are shown in Figure 3, and are divided into solids, liquids, and the major gases of CH_4, CO, CO_2 and H_2. In all cases, the solid yield dominated the liquid and gas fractions and mass balance closure was $> 95\,\%$, except for torrefaction at 300°C and 270°C after 120 min pyrolysis of treatment. The char yield decreased with increasing temperature and residence time [72, 73]. Char yields of all olive stones fractions did not show significant differences in product yields in the temperature range from 200 to 270°C, indicating that the degree of torrefaction below 270°C is relatively small.

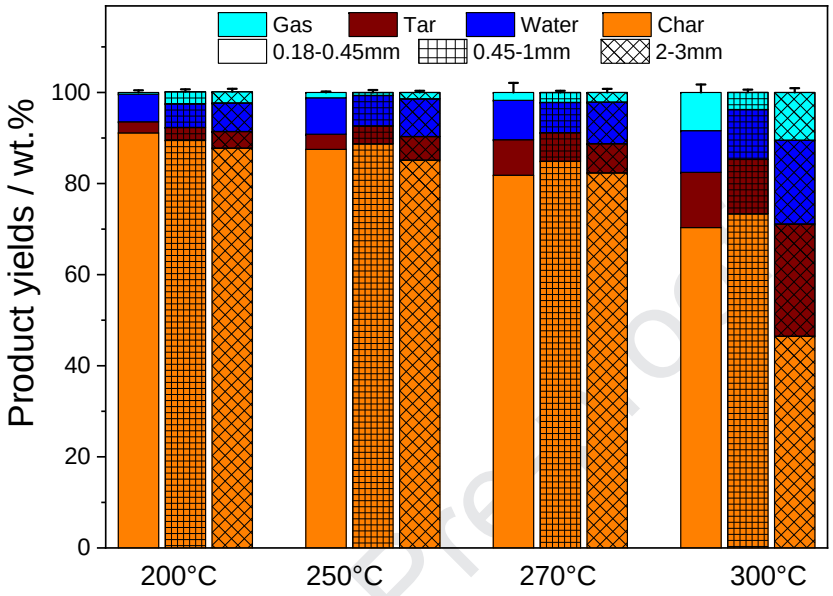

3(a):Product yields during torrefaction at 200, 250, 270 and 300°C

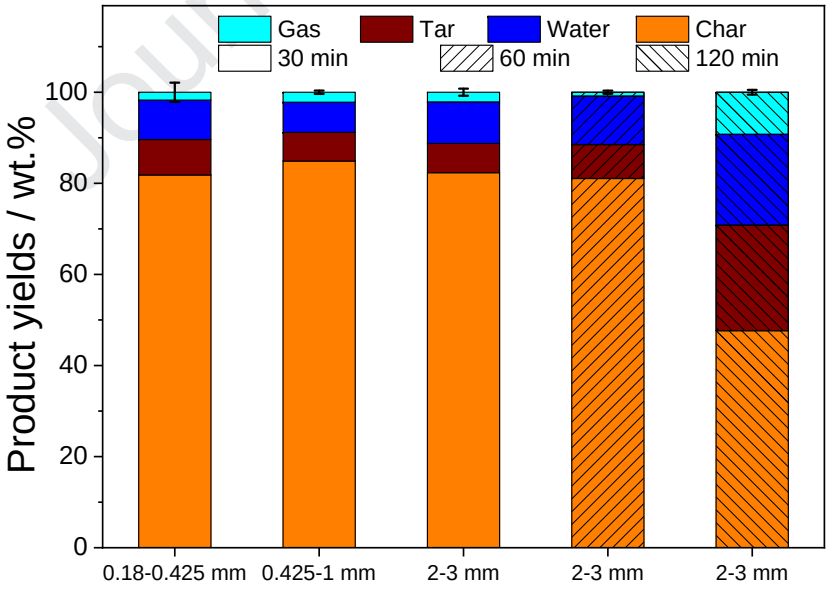

3(b):Product yield during torrefaction at 270°C

Figure 3: Product yields from torrefaction of (a) olive stone particles sieved to 0.18-0.425, 0.425-1 and 2-3 mm size fractions at 200, 250, 270 and 300°C reacted for 30 min and (b) at 270°C reacted for 30, 60 and 120 min.

Bates and Ghoniem showed that the composition of willow from torrefaction at temperatures less than 200°C is similar to that of the original feedstock, whereas higher temperatures led to an increase in the mass fraction of carbon and decreases in those of oxygen and hydrogen [74]. Torrefaction at 300°C showed a significant decrease in solid yield and an increase in gas, tar and water content for all particle size fractions. The difference in product yields from torrefaction of 0.18-0.425 and 0.425-1 mm particle fractions at 300°C was negligible, whereas torrefaction of 2-3 mm olive stones led to a decrease in solid yield from 70 to 45 % compared to other particle size fractions. This is due to the small temperature gradient inside particles of smaller than 1 mm during torrefaction, confirming the previous results of Peng et al. [75]. Particles larger than 2 mm give rise to an inter-particle vapor-char interaction, leading to an increase in tar fractions at 300°C as reported previously from torrefaction of wood [76, 77]. Prolongation of torrefaction time from 30 to 60 min did not influence product yields during pyrolysis at 270°C, whereas the residence time of 120 min led to a decrease in solid yield from 80 to 45 % and an increase in water, tar and gas yields, as shown in Figure 3(b). This highlights the relative importance of a long torrefaction time of 120 min and high heat treatment temperature of 300°C on the product yields. The torrefaction gas composition remains relatively unchanged at temperatures below 270°C, whereas more H_2, CH_4 and CO gases were formed at increased of residence time and heat treatment temperature, as shown in Figure 4.

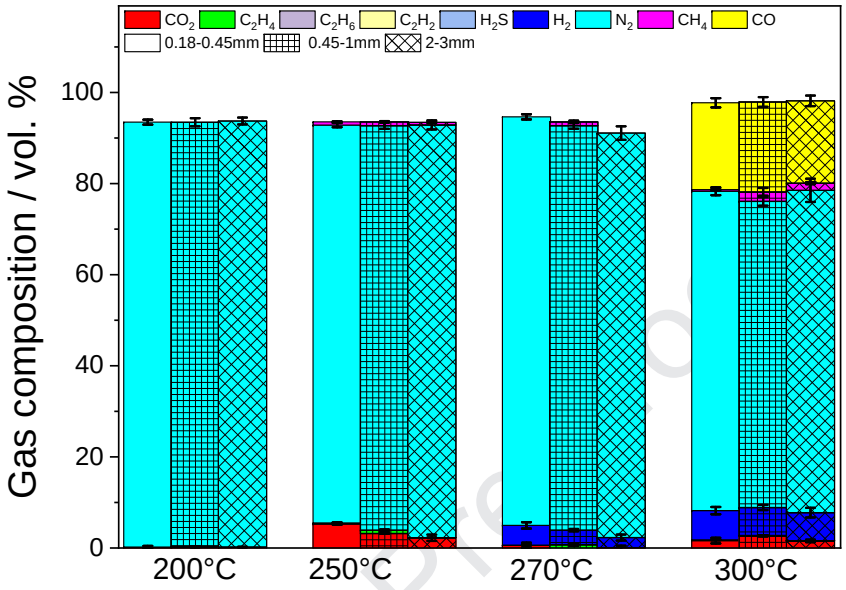

4(a):Gas yield during torrefaction at 200, 250, 270 and 300°C

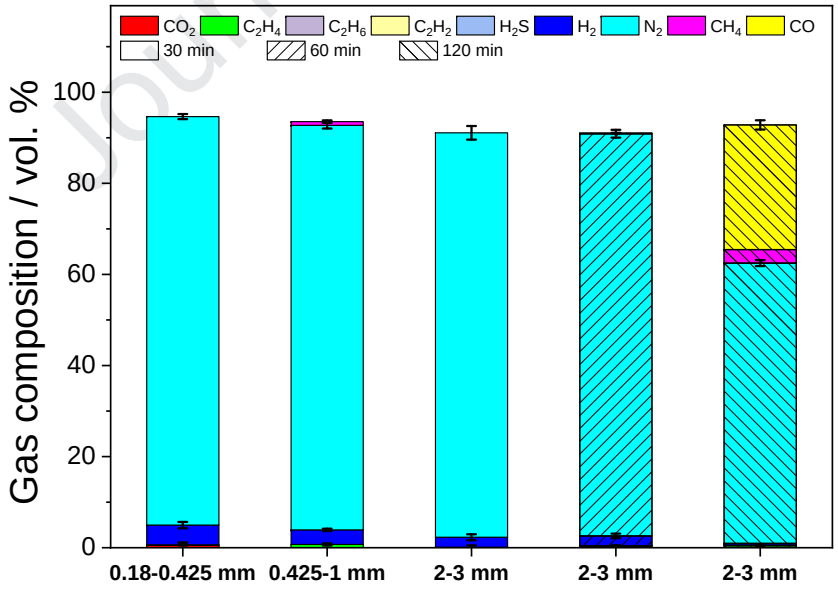

4(b):Gas yield during torrefaction at 270°C

Figure 4: Gas yields from torrefaction of (a) olive stone particles sieved to 0.18-0.425, 0.425-1 and 2-3 mm size fractions at 200, 250, 270 and 300°C reacted for 30 min and (b) at 270°C reacted for 30, 60 and 120 min.

The yield of gas at temperatures from 200 to 270°C and residence time of 30 min was 0.4-1.7 wt. %, it increased up to about 9.3 wt. %, at 270°C during torrefaction for 120 min and up to about 8.4 wt. % at 300°C reacted for 30 min, as shown in the supplemental material (Table S-3). The gas composition corresponds well with the decomposition of the chemical constituents of olive stones during torrefaction. Previous studies have shown that hemicellulose decomposition resulted in higher CO_2 yield, cellulose generated higher CO yield, and lignin gave higher H_2 and CH_4 yield [78]. At 200°C only negligible amounts of CO_2 were released from all samples, as shown in Figure 4(a), and hemicellulose only started to decompose (see Table 2). At 250°C the amount of CO_2 released increased to 3-6 wt. %. Moreover, very small amounts of H_2 and CO were released as well, and cellulose only started to decompose while hemicellulose decomposition continued. At 270°C mainly H_2 was released at 2-5 wt. %, and lignin only started to decompose (Table 2 and Figure S-2). When the residence time was extended to 120 min even at 270°C in addition to H_2, CO and CH_4 were also released. At 300°C CO was the main gaseous product, together with some H_2, CO_2 and CH_4. The calorific value of the torrefaction gas increased from 0.25 to 3.2 MJ Nm^{-3} when the residence time and heat treatment temperature were set to 120 min and 300°C, as shown in the supplemental material (Figure S-5). Heat treatment temperatures higher than 270°C and torrefaction times greater than 30 min are the optimum conditions for the torrefaction of olive stones at laboratory and pilot plant scale, confirming previous results in the literature [1, 47].

3.4. Higher heating value

A comparison of higher heating values (HHV) determined for raw and torrefied olive stone samples showed that the HHV increased during torrefaction, as presented in Table 2. Torrefaction of olive stones at temperatures below 300°C led to only a slight increase in HHV, in contrast to results obtained for willow or miscanthus [79]. Torrefaction of 2-3 mm particles at 270°C for 120 min led to the greatest HHV compared to torrefaction of olive stones at other operating conditions. This indicates that olive stones are more difficult to process due to their intrinsic properties (hardness/density).

Table 2: High heating values of 0.18-0.425, 0.425-1 and 2-3 mm torrefied olive stones from pyrolysis at 200, 250, 270 and 300°C with the residence time of 30 min and at 270°C with residence times of 45, 60 and 120 min (MJ kg^{-1}).

Condition	**0.18-0.425 mm**		**0.425-1 mm**		**2-3 mm**	
	HHV	**LHV**	**HHV**	**LHV**	**HHV**	**LHV**
raw	20.3	18.7	19.7	18.2	19.5	18.0
200°C, 30 min	21.4	20.2	20.5	19.3	20.3	19.1
250°C, 30 min	21.9	20.8	21.2	19.9	20.7	19.6
270°C, 30 min	22.5	21.3	21.6	20.5	21.4	20.2
300°C, 30 min	23.0	21.9	22.5	21.4	22.1	21.0
270°C, 45 min					21.7	20.6
270°C, 60 min					22.3	21.2
270°C, 120 min					22.6	21.5

The higher heating values of torrefied olive stones were in the range of 20.3 to 23.0 MJ kg^{-1} which are similar to those of peat (21.2 MJ kg^{-1}) and sub-bituminous coal (24 MJ kg^{-1}) used for heat and power generation [80, 81]. The higher heating value of olive stones torrefied in a laboratory scale reactor

was similar to those of briquettes generated at Arigna Fuels using torrefied olive stones and coal and 19 % starch binder or briquettes prepared with coal using double the amount of binder and containing torrefied woodchips (22.9 MJ kg^{-1}) [1]. The results show that the amount of binder had only a slight effect on the calorific value of torrefied olive stone briquettes. The calorific value of torrefied feedstocks could be increased by the design of a laboratory scale reactor that permits the permanent mixing of particles during torrefaction due to the improvement of the heat transfer inside the olive stone particles, as suggested by Medic [63, 82].

3.5. FTIR

FTIR analysis was conducted to investigate the changes in the main functional groups in a carbonaceous matrix of torrefied olive stones. The FTIR spectra with multiple bands of untreated and torrefied olive stones are shown in Figures 5-6 and the assignment of major bands is reported in the supplemental material (Table S-2) [83–90]. Differences between the original feedstock and torrefied olive stones mainly appeared in the spectral range 1020 to 1850 cm^{-1}. Torrefaction of olive stones resulted in a disappearance of the band at 1654 cm^{-1} originating from the stretching vibrations of C=O in conjugated p-substituted aryl ketones [83]. Moreover, an increase in the torrefaction temperature from 200 to 300°C led to the formation of band at 1270 cm^{-1} that was assigned to the stretching of C=O group [83, 84].

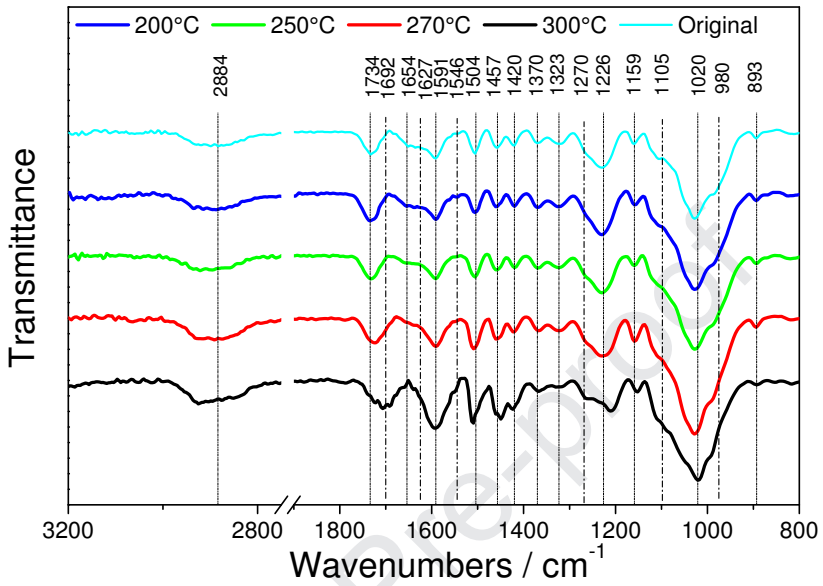

5(a):0-0.18 mm torrefied olive stones

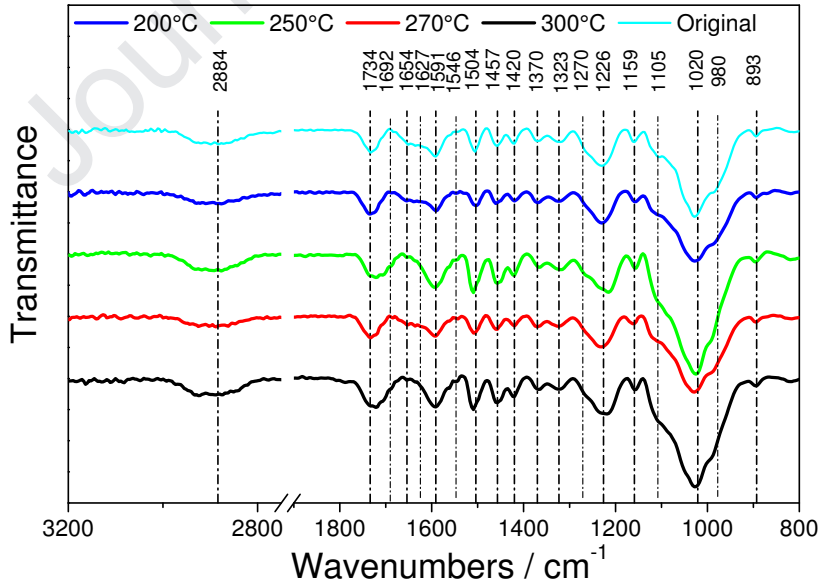

5(b):0.18-0.425 mm torrefied olive stones

Figure 5: Experimental IR spectra of (a) 0.18-0.425 mm torrefied olive stones; (b) 0.425-1 mm torrefied olive stones produced at 200, 250, 270 and 300°C reacted for 30 min.

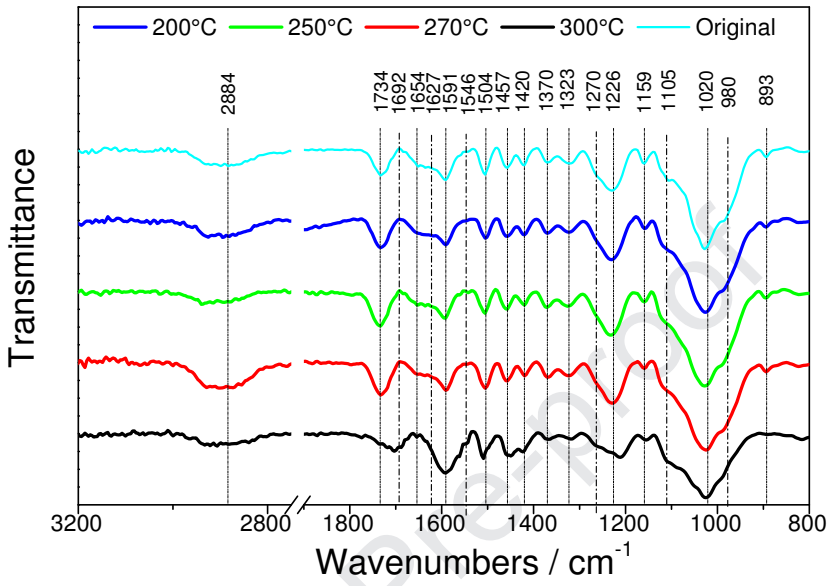

6(a):2-3 mm torrefied olive stones (200, 250, 270, 300°C)

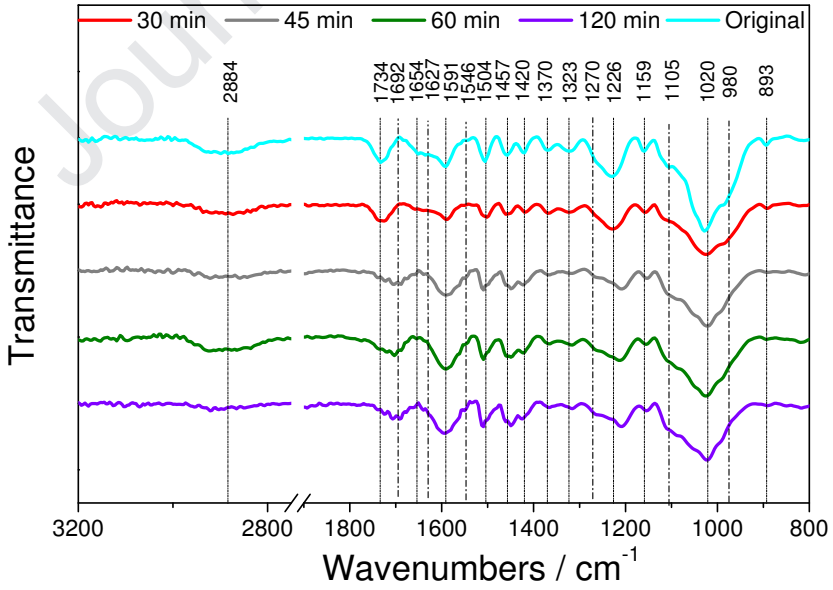

6(b):2-3 mm torrefied olive stones at 270°C (30, 45, 60, 120 min)

Figure 6: Experimental IR spectra of (a) 2-3 mm torrefied olive stones produced at 200, 250, 270 and 300°C reacted for 30 min; (b) 2-3 mm torrefied olive stones produced at 270°C reacted for 30, 45, 60 and 120 min.

This is likely due to the decomposition of hemicellulose at temperatures $> 220°C$ and conversion of cellulose into hexose and oligosaccharides at temperatures above 230°C [91, 92]. A similar trend was noted for the increase in torrefaction time leading to the formation of C=O groups in the carbonaceous matrix of olive stones. Moreover, the C-O peak disappeared with the increased torrefaction time indicating the formation of mostly polyaromatic structures [93]. Interestingly, the intensity of the NH bending increased with longer torrefaction times indicating the increased ability of biochars to adsorb NH_4^+-N and NO_3^--N [94, 95]. FTIR analysis showed that the chemical composition of different particle size fractions during torrefaction is similar.

3.6. ToF-SIMS

Torrefied olive stones were studied using the ToF-SIMS technique in order to determine surface compositional changes during thermal treatment. Figures 7(a), 7(c) and 7(e) show differences in the intensity of selected low mass negative ions (C_2HO^-, CHO_2^-, $C_2H_2O_2^-$ and $C_2H_3O_2^-$; m/z = 41, 45, 58 and 59, respectively). These ions come from the principal components of olive stones and changes of intensity allow for comparison of total O, H and C content on the surface of torrefied samples. However, due to their relatively simple structure and possibility of fragmentation of complex molecules during the experiments they cannot be univocally assigned to specific molecules [59, 96]. The results demonstrate that regardless of particle size, the largest decrease in the intensity of the aforementioned secondary ions is observed for the materials subjected to torrefaction above 250°C, whereas the changes in the intensity noted up to this temperature were not significant.

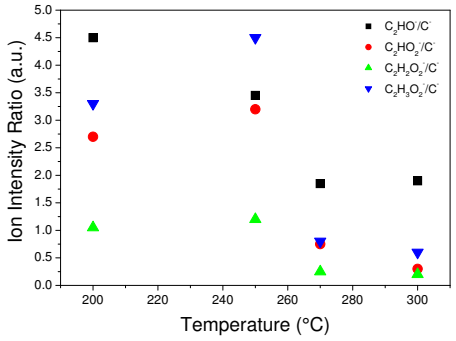

7(a):N. I. of negative ions (0.18-0.425 mm)

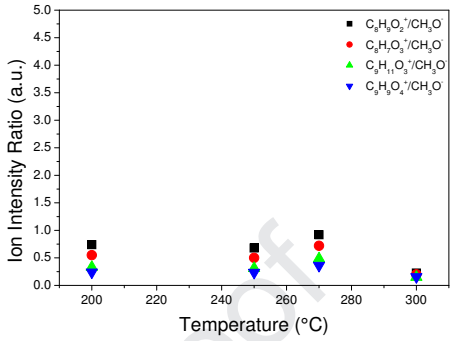

7(b):N. I. of positive ions (0.18-0.425 mm)

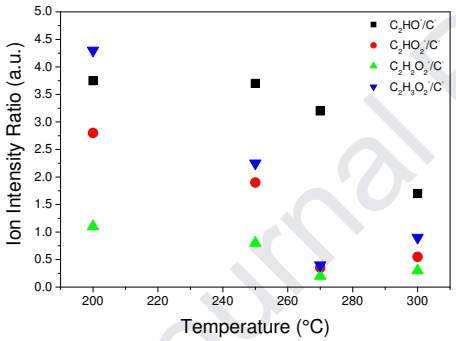

7(c):N. I. of negative ions (0.425-1 mm)

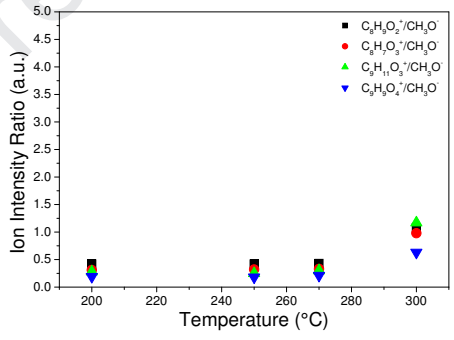

7(d):N. I. of positive ions (0.425-1 mm)

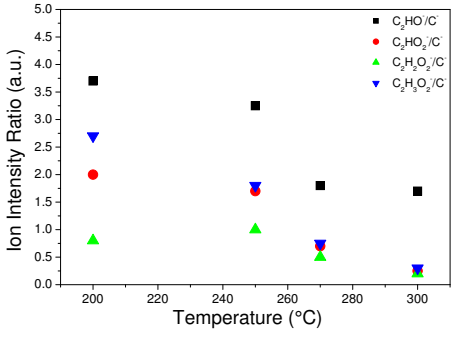

7(e):N. I. of negative ions (2-3 mm)

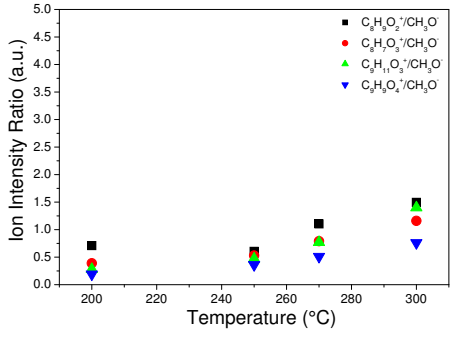

7(f):N. I. of positive ions (2-3 mm)

Figure 7: Normalized intensity (N. I.) of selected negative and positive ions calculated from mass spectra collected from the surface of original olive stones and solid residue of particle size 0.18-0.425, 0.425-1 and 2-3 mm from the treatment at 200, 250, 270 and 300°C reacted for 30 min.

An increase in the temperature from 270 to 300°C did not influence the strength of the ToF-SIMS signals. This suggests that the most intense removal of H and O from the surface of torrefied olive stones, evidenced by the drop of the values of $C_xH_yO_z^-/C$ intensity ratios takes place between 250°C and 270°C. A further increase in torrefaction temperature does not impact the relation between the amounts of H, O and C in the upper layer of the investigated samples. However, successive decomposition of the biomass components in the bulk may be observed at higher temperature, as mentioned earlier. Figure 8 shows a comparison of the influence of time on the olive stone compositional changes during pyrolysis. It seems that 270°C process conditions for 60 min led to the decrease in the intensity of low mass negative ions. This suggests that the upper layers of the torrefied material become richer in carbon with the extension of reaction time. The intensities of complex secondary ions assigned to the presence of cellulose and lignin were compared [59, 60, 97, 98]. In spite of the problems related to the non-conductive character and fibrous structure of the analyzed material literature reports [99–101] and our previous studies [96] demonstrated that ToF-SIMS analysis allows for the estimation of specific lignocellulosic components content on the surface of biomass samples subjected to thermal treatment. In the present investigations we focused on the estimation of change in the contribution of cellulose and lignin that occurred during torrefaction. In order to do that the intensity ratios between ions originating from lignin (numerator) and ion coming from cellulose (denominator) were calculated.

Figures 7(b), 7(d) and 7(f) show that heating of olive stones up to 250°C for 30 min did not change the surface contribution of cellulose and lignin

observed for torrefied olive stones. The ratios of cellulose combined with hemicellulose and lignin (C+H/L = 1.48, 1.38, 1.41) in torrefied 2-3 mm olive stones remained only slightly changed up to 270°C based on the chemical analysis, as shown in Table 3. A further increase in the heat treatment temperature resulted in the increase in surface content of lignin, which was the highest for the samples treated at 300°C (taking into account materials with average and the largest particle size). In addition, the most significant changes in the chemical composition (C+H/L = 0.63 and 0.75) were observed in the torrefied material from 300°C for 30 min and 270°C for 60 min, as shown in Table 3. This is in line with literature descriptions reporting that cellulose is more prone to thermal decomposition than lignin [78], as is also presented in the results of our previous investigations [96]. The exception is the sample with the smallest grain size (0.18-0.425 mm). In this case the analyzed ion intensity ratios initially increased (with the maximum at 270°C), but then decreased reaching the minimum at 300°C, as shown in Figure 7(b). Small olive stone particles exhibit a lower conduction resistance and thus a greater heat flux than large particles. Therefore, heavy molecular compounds on the surface of small olive stones are more effectively converted to small molecular products, confirming the results of Deng et al. [102].

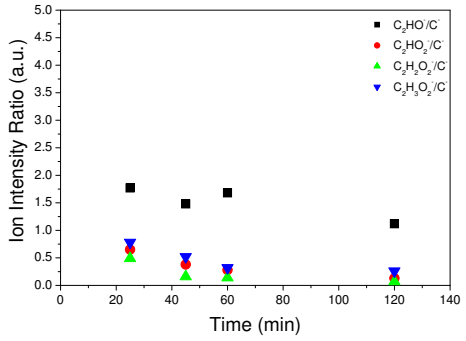

8(a):Normalized intensity of negative ions

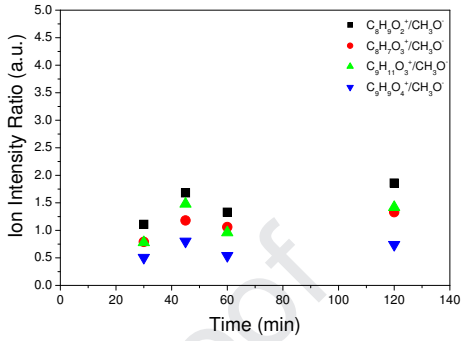

8(b):Normalized intensity of positive ions

Figure 8: Normalized intensity of selected negative and positive ions calculated on the basis of the mass spectra collected from the surface of original olive stones and solid residue from the treatment at 270°C reacted for 30, 45, 60 and 120 min.

Further measurements demonstrated that an increase in torrefaction time resulted in the growth in lignin/cellulose ratio, as shown in Figure 8. This growth was observed for material reacted over 60 min, which confirms more efficient decomposition of cellulose. The observed increase in lignin/cellulose intensity ratio was accompanied by a decrease in the O and H surface content, indicating that the decomposition products containing these elements are removed from the upper layer of the studied sample during torrefaction.

3.7. Elemental analysis

Figure 9 shows a van Krevelen plot of original feedstock and torrefied olive stone samples. Increasing the reaction time to 120 min led to the decrease in H/C ratio, consistent with decomposition of cellulose and hemi-

cellulose and formation of polyaromatic char structure, confirming previous results [103, 104]. In addition, a van Krevelen plot of torrefied material demonstrates that the oxygen and hydrogen content mostly decreased with the increased heat treatment temperature and longer residence times, corresponding to the ToF-SIMS results. Figure 9 indicated the elemental composition of torrefied olive stones was mostly modified under the highest heat treatment of 300°C for 30 min and at 270°C with residence times from 45 to 120 min leading to the formation of solid residue of similar chemical structure. Moreover, the elemental composition of olive stones from torrefaction at temperatures below 270°C shows that the chemical structure is similar to that of the original feedstock.

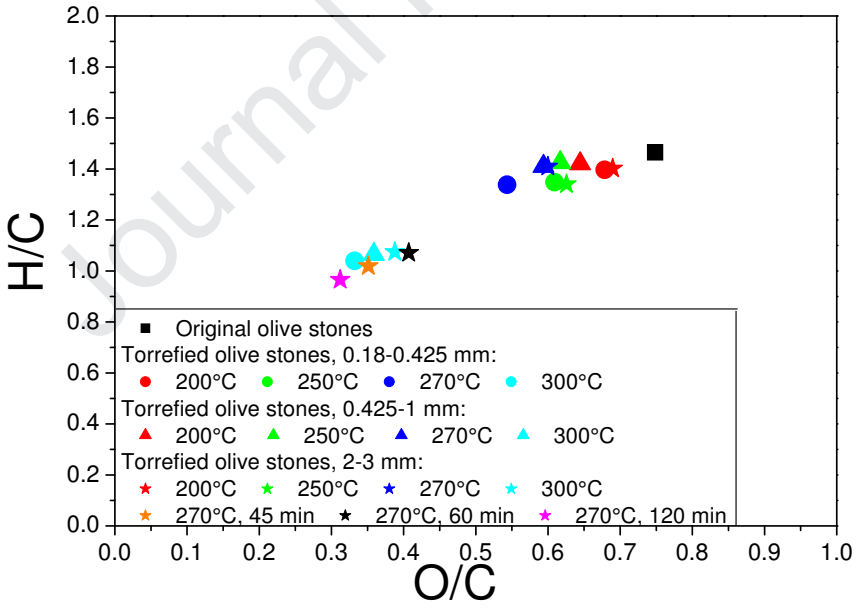

Figure 9: Van Krevelen diagram of olive stone particles sieved to 0.18-0.425, 0.425-1 and 2-3 mm size fractions and reacted at 200, 250, 270 and 300°C during 30, 60 and 120 min.

3.8. Bulk thermal conductivity

The characterisation of the bulk thermal conductivity of original olives stones and torrefied material was carried out using the test apparatus constructed in-house described above. Gravel, rice grains, granulated sugar and plain flour were used to calibrate the bulk thermal conductivity apparatus. These calibration materials were chosen due to their similar granular structure and particle size to the biomass being tested [105]. Olive stones with varying countries of origin, moisture content, and particle size were used to understand the effect of feedstock on the thermal properties of biomass and torrefied material. The torrefied olive stones were generated at 280°C at the Arigna Fuels torrefaction plant, as described previously [1]. Figure 10 shows that the thermal conductivity values vary from 0.15 to 0.33 W $m^{-1}K^{-1}$, confirming results in the literature [106–108].

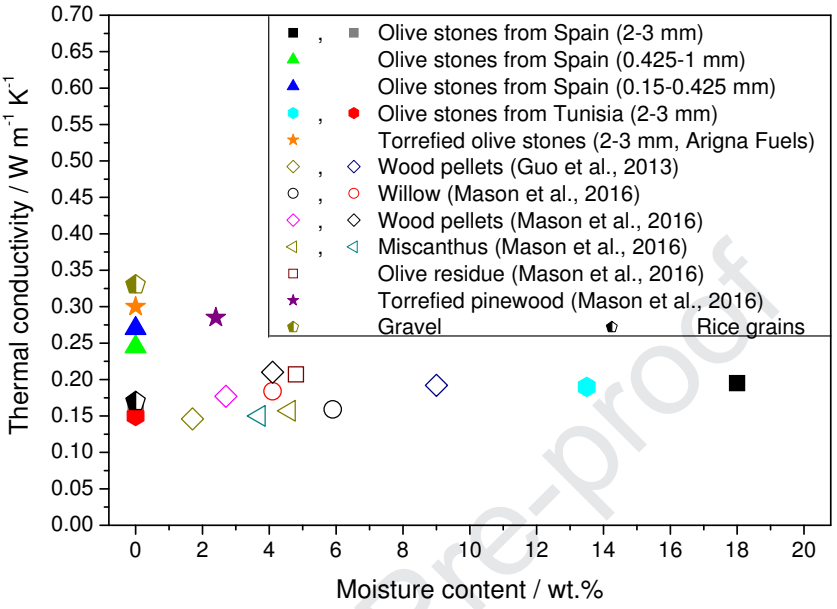

Figure 10: Bulk thermal conductivity values of gravel, rice grains, olive stone particles from Tunisia and Spain sieved to 0.15-0.425, 0.425-1 and 2-3 mm size fractions, which contain 0, 13.5 and 18 % moisture and olive stones torrefied at 280°C at Arigna Fuel pilot plant compared with the literature data [106, 107, 109].

In order to analyse trends in thermal conductivity relating to the moisture content of the biomass, the Spanish olive stones with 18 % moisture content and Tunisian olive stones with 13.5 % moisture content were both dried out using an oven. The results showed that an increase in the moisture content of olive stones correlates with an increase in bulk thermal conductivity. An increase in the moisture content of olive stones correlates well with an increase in thermal conductivity. The results also showed that increasing particle size gives a decrease in thermal conductivity due to increased volume of air gaps between olive stone particles. With increasing particle size,

the fraction of air in the sample volume is increased due to larger pockets between particles. The conductivity of air is approximately 0.025 W $m^{-1}K^{-1}$ at room temperature, which is significantly lower than the conductivity of biomass particles [110]. Thus, by increasing the particle size, the amount of air in the sample is increased, decreasing the bulk thermal conductivity. Moreover, this study showed that thermal conductivity values of dried olive stones from Tunisia and Spain were similar, indicating a similar cross-grain structure in both biomass samples. Figure 10 shows that the previously reported thermal conductivity values of a range of biomass fuels such as wood, straw and wood pellets can range from 0.15 to 0.28 W $m^{-1}K^{-1}$ using steady state methods [107]. Another study [108] showed that the bulk thermal conductivity of various types of barley with a range of moisture contents obtained thermal conductivity values in a range from 0.193 to 0.288 W $m^{-1}K^{-1}$ using the transient line heat source method [107].

Comparison of present experimental results with the literature results shows that despite the difference in thermal conductivity test methods, similar ranges of conductivity values are observed [108]. Torrefied olive stones are also shown to have a 55 % greater bulk thermal conductivity than raw olive stones. The thermal conductivity value of torrefied pinewood (0.33 W $m^{-1}K^{-1}$) from the literature was slightly greater than that of torrefied olive stones (0.3 W $m^{-1}K^{-1}$), probably due to the lower bulk density of torrefied pinewood (0.45 g cm^{-3}) [107]. In addition, the thermal conductivity of torrefied olive stones was below the explosive limits of solid fuels i.e. PTFE ($<$ 0.38 W $m^{-1}K^{-1}$) [111]. This shows that the torrefaction process at temperatures below 300°C does not contain any risks related to material self-heating,

thermal runaway and fire ignition at large-scale plant. In general, it is expected that the difference in thermal conductivity values of both torrefied biomass samples are small due to the similar cross-grain fiber orientation in non-treated olive residues and wood [109].

3.9. Thermogravimetric analysis

Figure 11 shows differential weight loss curves (DTG) in 20 % volume fraction O_2 and 20 % volume fraction CO_2 gasification for 0.18-0.425 and 2-3 mm torrefied olive stone fractions. The DTG curves of 0.425-1 mm torrefied olive stones are shown in the supplemental material (Figure S-1). Depending on the sample, the DTG curves show both either a single broad peak or a double peak in the temperature range 200 to 600°C which is referred to the pyrolysis process. Both peaks indicate a heterogeneous char mixture with respect to reactivity [103, 112]. Oxidation of torrefied olive stones took place in the temperature range 400 to 550°C with a peak at a temperature of approximately 510°C and CO_2 gasification in the temperature range 700 to 1010°C with a peak temperature of approximately 950°C. An initial mass loss from olive stones torrefied at 200 and 250°C occurred at 200°C with a peak temperature of 260°C. The chemical composition of 2-3 mm olive stones is shown in Table 3. Data presented in Figure 11(c) indicates that the first peak of large torrefied olive stones processed at 300°C and 30 min residence time has diminished during oxidation. Thus, a single broad peak corresponding to oxidation and CO_2 gasification experiments has been formed. Table 3 shows that the gradual changes in the chemical composition of olive stones mainly occurred during torrefaction at 300°C with the reduction in hemicellulose and cellulose content from 25.6 to 4.6 % and from 25.4 to 10.8 % respectively.

Table 3: Calculated content (in g) of Cellulose (C), Hemicellulose (H), Lignin acid-soluble (LA), Lignin acid-insoluble (LAI) and Extractives (E) for 100 g of 2-3 mm original and torrefied olive stones. HPLC and wet chemical analysis according to NREL technical reports [113–115] and Thammasouk et al. [116],

Condition	**Yield**	**C**	**H**	**LA**	**LAI**	**E**
raw	100	25.4	25.6	28.9	1.6	3
200°C, 30 min	87.8	20.7	23.2	27.8	1.7	2.6
250°C, 30 min	85.1	19.1	21.2	27.7	1.5	3.5
270°C, 30 min	82.3	19.9	19.9	26.7	1.4	4.2
300°C, 30 min	46.5	10.8	4.6	24.2	0.2	3.7
270°C, 60 min	78.5	19.4	7.9	35.9	0.5	9.6

Thus, the first peak of torrefied biomass from treatment below 270°C during oxidation and CO_2 gasification is attributed to the decomposition of hemicellulose. The second peak denotes the breakdown of cellulose because the changes in composition of torrefied olive stones are minor at temperatures of 270°C or below. The torrefaction temperature had a strong influence on lignin leading to a content decrease from 30.5 to 24.4 % when it was increased to 300°C. Interestingly, the major change in O_2 and CO_2 reactivity was mainly found for the olive stones which were torrefied at 300°C with a peak temperature at 310°C during pyrolysis stage and with a peak temperature of 500°C during oxidation. During CO_2 gasification, the DTG peak of olive stones from torrefaction at 300°C was only one single broad peak and the gasification peak had peak temperatures ranging from 950 to 970°C.

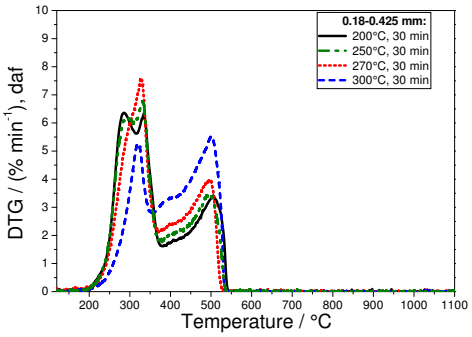

11(a):0.18-0.425 mm, 20 % O_2

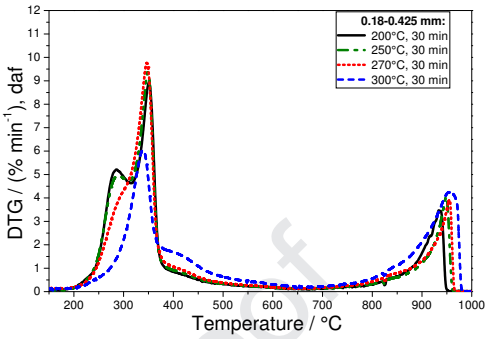

11(b):0.18-0.425 mm, 20 % CO_2

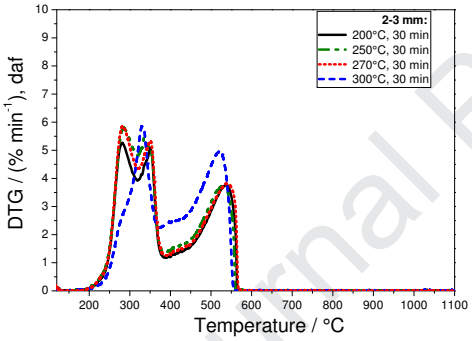

11(c):2-3 mm, 20 % O_2

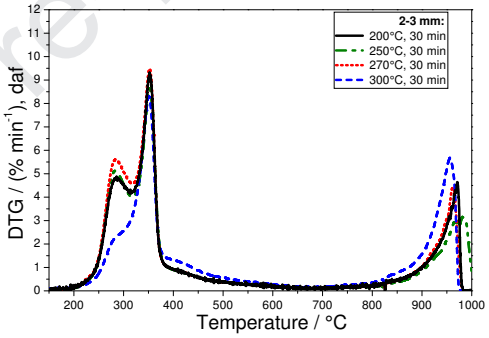

11(d):2-3 mm, 20 % CO_2

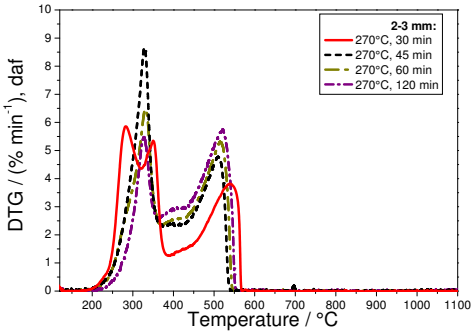

11(e): -3 mm, 20 % O_2 (30, 45, 60, 120 min)

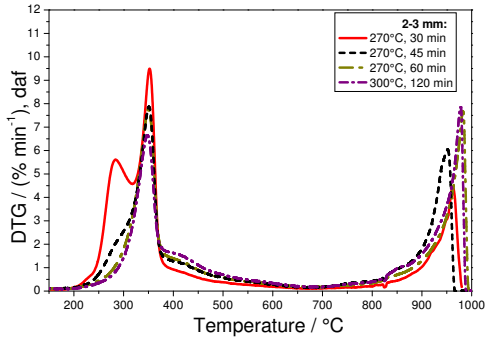

11(f): -3 mm, 20 % CO_2 (30, 45, 60, 120 min)

Figure 11: DTG curves of torrefied olive stones of size 0.18-0.425 and 2-3 mm prepared at 200, 250, 270 and 300°C with 30 min residence time and at 270°C with 30, 45, 60 and 120 min residence time and further reacted in 20 % volume fraction O_2 + 80 % volume fraction N_2 or 20 % volume fraction CO_2 + 80 % volume fraction N_2.

The residence time of torrefied olive stones had a negligible influence on the CO_2 reactivity leading to the peak temperature shift from 940 to 975°C when the residence time was increased from 30 to 120 min. Kinetic analysis in the supplemental material (Table S-5 and S-6) showed that the torrefied olive stones obtained from pyrolysis at 270°C, residence 30 min have the same O_2 and CO_2 reactivity as the torrefied samples from pyrolysis at longer times.

4. Discussion

The results of this work demonstrated that the use of solid agriwaste has the potential to produce high-quality briquettes for the energy sector with a pilot plant efficiency greater than 90 %. The use of olive stones from a three phase extraction process generates feedstocks with the moisture content less than 50 %. However, the favourable climate in Tunisia decreases the moisture content of olive stones to less than 20 % due to natural evaporation. This is of a great benefit to the torrefaction process at Arigna Fuels decreasing the requirement for pre-drying. Compared to the lower calorific value of torrefied feedstock with about 19 % of starch binder in each individual coal-biomass briquette [1], the calorific values of torrefied olive stone fractions did not vary significantly with the feed particle size.

Differences in lignocellulosic composition and ash content, heat treatment temperature and residence time exerted a significant influence on the intrinsic reactivity and composition of torrefied material. Olive stones of particle size less than 0.425 mm exhibited more cellulose than lignin on the surface in comparison to the material consisted of larger grains. In addition, olive stones of particle size less than 0.425 mm torrefied at 300°C for 30 min

contain much less hemicellulose but more cellulose than raw biomass. High cellulose-containing biomass elevates the burning temperature and longevity of briquettes in a woodstove [117, 118]. Thus, the cellulose lean (7.9 wt. %) and lignin rich (36.3 wt. %) olive stones after torrefaction at 270°C for 60 min can oxidize faster in a woodstove due to the more highly carbonized structure with the less alkali metals than olive stones from torrefaction at low temperatures and residence times. In addition, the present work demonstrated that the O_2/CO_2 reactivity of torrefied material was affected equally by both the organic and inorganic components of olive stones. On the one hand, the shrinking of one of the DTG peaks during pyrolysis stage of thermogravimetric analysis indicated decomposition of hemicellulose and repolymerization of lignin and remaining residue of cellulose, leading to the decrease in reactivity with the increasing heat treatment temperature and longer residence time. On the other hand, the calcium content in small particles (0.18-0.425 mm) was at least 50 % greater than in large particles at torrefaction temperatures from 270 to 300°C, whereas the CO_2 reactivity of small torrefied olive stones was at least double that of the 2-3 mm torrefied material. The difference in ash composition among the different particle size fractions was related to the milling of the original olive stones. Small particles arising from the breakage of brittle tissues of inorganic rich large particles showed high ash content [119]. Thus, high amount of alkali metals in olive stone particles of smaller size could promote faster devolatilization rates and suppress tar formation, leading to higher solid product yields and higher CO_2/O_2 reactivity of torrefied material than low-ash containing feedstocks [120].

In general, the product yields from torrefaction of olive stones indicated

that temperatures above 270°C lead to a significant decrease in solid product yield compared the treatment at low temperatures, especially for olive stones of particle size greater than 0.425 mm. Operation of a torrefaction plant will require temperatures in the range 270 to 300°C and particle size below 2 mm to obtain the maximum solid product yield and thermal conductivity values below 0.38 W $m^{-1}K^{-1}$. A recent study reported that feedstock composition has an effect on liquid product formation during oxidation and gasification of briquettes from torrefied biomass [121]. Extended torrefaction times may also significantly decrease the yields of solid char and increase the formation of undesired liquid products which will negatively affect the energy balance on a large scale [36, 122, 123]. Therefore, the pretreatment of olive stones under the suggested conditions might be more suitable for the production of biomass briquettes than torrefaction of olive stones of size larger than 2 mm at temperatures less than 270°C and residence time longer than 30 min to achieve energy efficiency of at least 65 %.

5. Conclusion

The main finding of this study was that at pilot scale operation olive stones of size less than 2 mm from torrefaction at 270°C for 30 min are the most suitable material for briquetting with coal due to the high solid char yield, low reactivity and more favourable thermal conductivity values. Thermogravimetric analysis showed that both the inorganic matter and lignocellulosic composition of the original olive stones had an equal effect on the intrinsic reactivity of torrefied material. Size reduction of olive stones led to the higher ash content in small particles and thus, the concentration

of calcium was also greater than in large olive stones. ToF-SIMS results showed that olive stones of size less than 0.425 mm contained more cellulose than lignin on the particle surface in comparison to the material consisted of larger grains. Torrefaction of olive stones shows great promise for producing torrefied biomass briquettes with calorific values comparable to peat and thermal conductivity values below explosive limits of solid fuels. The findings of this study emphasize the potential use of torrefied olive stones in the energy sector, with concomitant reduction in CO_2 emissions.

Acknowledgements

The authors gratefully acknowledge financial support from the Science Foundation Ireland (Grant number 16/SP/3829) and Arigna Fuels under the Sustainable Energy and Fuel Efficiency (SEFE) spoke of the Research Centre for Marine and Renewable Energy (MaREI). Dr. Gerrit Ralf Surup from NTNU and Dr. Daniel Hayes from Celignis are acknowledged for the technical support on thermogravimetric measurements and analysis of lignocellulosic composition. Master students from NUI Galway Mechanical Engineering, Dara Nashat, and Thomas Deric, and Sary Fayed from American University of Beirut are acknowledged for the construction of thermal conductivity rig and help with the experimental campaign using a slow pyrolysis reactor respectively.

[1] Trubetskaya A, Leahy JJ, Johnson R, Layden P, Müller M, Monaghan RFD and etc., Characterization of woodstove briquettes from torrefied biomass and coal, Energy 171 (2019) 853–65.

[2] Mulligan CJ, Strezov L, Strezov V, Thermal Decomposition of Wheat Straw and Mallee Residue Under Pyrolysis Conditions, Energy Fuels 24 (2019) 46–52.

[3] Wang Y, Qiu L, Zhu M, Sun G, Zhang T, Kang K, Comparative Evaluation of Hydrothermal Carbonization and Low Temperature Pyrolysis of Eucommia ulmoides Oliver for the Production of Solid Biofuel, Sci Rep 9 (5535) (2019) 1–11.

[4] Bullock C, Hawe J, Little D, Realising the ecosystem-service value of native woodland in Ireland, New Zeal J Forest Sci 44 (2014) 1–10.

[5] Williams PT, Nugranad N, Comparison of products from the pyrolysis and catalytic pyrolysis of rice husks, Energy 25 (2000) 493–513.

[6] Pawelczyk A, EU policy and legislation on recycling of organic wastes to agriculture, ISAH 1 (2005) 64–71.

[7] Trubetskaya A, Jensen PA, Jensen AD, Steibel M, Spliethoff H, Glarborg P, Hofmann Larsen F, Comparison of high temperature chars of wheat straw and rice husk with respect to chemistry, morphology and reactivity, Biomass Bioenergy 86 (2016) 76–87.

[8] Benavente V, Fullana A, Torrefaction of olive mill waste, Biomass Bioenergy 73 (2015) 186–94.

[9] Uribe E, Lemus-Mondaca R, Pasten A, Astudillo S, Vega-Galvez A, Puente-Diaz L and etc., Dehydrated olive-waste cake as a source of high value-added bioproduct: Drying kinetics, physicochemical properties, and bioactive compounds, Chilean J Agric Res 74 (3) (2014) 293–301.

[10] Manzanares P, Ruiz E, Ballesteros M, Negro MJ, Gallego FJ, Lopez-Linares JC and etc., Residual biomass potential in olive tree cultivation and olive oil industry in Spain: valorization proposal in a biorefinery context, Span J Agricult Res 15 (3) (2017) 1–12.

[11] Spinelli R, Picchi G, Industrial harvesting of olive tree pruning residue for energy biomass, Biores Tech 101 (2010) 730–5.

[12] Gonzalez-Garcia S, Gullon B, Rivas S, Feijoo G, Moreira MT, Environmental performace of biomass refining into high-added value compounds, J Cleaner Prod 120 (2016) 170–80.

[13] FitzPatrick M, Champagne P, Cunningham MF, Whitney RA, A biorefinery processing perspective: Treatment of lignocellulosic materials for the production of value-added products, Biores Technol 101 (2010) 8915–22.

[14] Calatrava J, Franco JA, Using pruning residues as mulch: Analysis of its adoption and process of diffusion in Southern Spain olive orchards, J Environ Manage 92 (2011) 620–9.

[15] Aparicio J, Monge JF, Ortiz L, Pastor JT, Changes in productivitiy in the virgin olive oil sector: An application to Protected Designations of Origin in Spain, Span J Agric Res 14 (3) (2016) 1–12.

[16] Vlyssides AG, Loizidou M, Gimouhopoulos K, Zorpas A, Olive oil processing wastes production and their characteristics in relation to olive oil extraction methods, Fres Envir Bull 7 (1998) 308–13.

[17] Spinelli R, Picchi G, Review and Analysis of Alternatives for the Valorisation of Agro-Industrial Olive Oil By-Products, Sustain 10 (237) (2018) 1–9.

[18] Alburquerque JA, Gonzalvez J, Garcia D, Cegarra J, Agrochemical characterization of "alperujo", a solid by-product of the two phase centrifugation method for olive oil extraction, Biores Tech 92 (2004) 195–200.

[19] Kapellakis IE, Tsagarakis KP, Crowther JC, Olive oil history, production and by-product management, Rev Env Sci Biotech 7 (2008) 1–26.

[20] Markou G, Geoergakakis D, Plagou K, Salakou G, Christopoulou N, Balanced Waste Management of 2- and 3-Phase Olive Oil Mills in Relation to the Seed Oil Extraction Plant, Terrest Aquatic Env Tox 4 (1) (2010) 109–12.

[21] Roig A, Cayuela ML, Sanchez-Monedero MA, An overview on olive mill wastes and their volarisation methods, Waste Manage 26 (2006) 960–9.

[22] Medic C, Darr M, Shah A, Potter B, Zimmermann J, Effects of torrefaction process parameters on biomass feedstock upgrading, Fuel 91 (1) (2012) 147–54.

[23] Cholewinski M, Kaminski M, Torrefaction as a Means to Increase the use of Solid Biomass for Power Generation and Heating, Acta Energetica 2 (27) (2016) 60–7.

[24] Hamid MF, Idroas MY, Ishak MZ, Zainal Alauddin ZA, Miskam MA, Abdullah MK, An Experimental Study of Briquetting Process of Torrefied Rubber Seed Kernel and Palm Oil Shell, Biomed Res Int 1 (2016) 1–11.

[25] Brscic K, Poljuha D, Krapac M, Olive residues - renewable source of energy, Sibenik, June 10-12 2009, Croatia, Management of Technology - Step to Sustainable Production .

[26] Nesvadba P, Methods for the measurement of thermal conductivity and diffusivity of foodstuffs, J Food Eng 1 (2) (1982) 93–113.

[27] Gonzalez Martinez M, Floquet P, Dupont C, Da Silva Perez D, Meyer XM, Assessing the impact of woody and agricultural biomass variability on its behaviour in torrefaction through Principal Component Analysis, Biomass Bioenergy 134 (2020) 105474.

[28] Zevenhoven-Onderwater M, Blomquist JP, Skrifvars BJ, Backman R, Hupa M, Prediction of behaviour of ashes from five different solid fuels in fluidised bed combustion, Fuel 79 (11) (2000) 1353–61.

[29] Werner K, Pommer L, Broström M, Thermal decomposition of hemicelluloses, J Anal Appl Pyrolysis 110 (2014) 130–7.

[30] Joffres B, Laurenti D, Charon N, Daudin A, Quignard A, Geantet C, Thermochemical conversion of lignin for fuels and chemicals: a review, Oil Gas Sci Tech 68 (2013) 753–63.

[31] Tsalidis GA, Di Marcello M, Spinelli G, de Jong W, Kiel JHA, The effect of torrefaction on the process performance of oxygen-steam blown CFB gasification of hardwood and softwood, Biomass Bioenergy 106 (2017) 155–65.

[32] Thrän D, Witt J, Schaubach K, Kiel J, Carbo M, Maier J and etc., Moving torrefaction towards market introduction - Technical improvements and economic-environmental assessment along the overall torrefaction supply chain through the SECTOR project, Biomass Bioenergy 89 (2016) 184–200.

[33] Shoulaifar TK, DeMartini N, Zevenhoven M, Verhoeff F, Kiel J, Hupa M, Ash-Forming Matter in Torrefied Birch Wood: Changes in Chemical Association, Energy Fuels 27 (2013) 5684–90.

[34] Couhert C, Salvador S, Commandre JM, Impact of torrefaction on syngas production from wood, Fuel 88 (11) (2009) 2286–90.

[35] Tsalidis GA, Voulgaris K, Anastasakis K, de Jong W, Kiel JHA, Influence of Torrefaction Pretreatment on Reactivity and Permanent Gas Formation during Devolatilization of Spruce, Energy Fuels 29 (9) (2015) 5825–34.

[36] Strandberg M, Olofsson I, Pommer L, Wiklund-Lindström S, Åberg K, Nordin A, Effects of temperature and residence time on continuous torrefaction of spruce wood, Fuel Process Tech 134 (2015) 387–98.

[37] Shang L, Ahrenfeldt J, Holm JK, Sanadi AR, Talbro Barsberg S, Thomsen T and etc., Changes of chemical and mechanical behavior of torrefied wheat straw, Biomass Bioenergy 40 (2012) 63–70.

[38] Li T, Geier MT, Wang L, Shaddix CR, Ku X, Matas Güell B and etc., Effect of Torrefaction on Physical Properties and Conversion Behavior of High Heating Rate Char of Forest Residue, Energy Fuels 29 (1) (2015) 177–84.

[39] Bajcar M, Zagula G, Saletnik B, Tarapatskyy M, Puchalski C, Relationship between Torrefaction Parameters and Physicochemical Properties of Torrefied Products Obtained from Selected Plant Biomass, Energies 11 (11) (2018) 1–13.

[40] Branca C, Di Blasi C, Galgano A, Broström M, Effects of the Torrefaction Conditions on the Fixed-Bed Pyrolysis of Norway Spruce, Energy Fuels 28 (9) (2014) 5882–91.

[41] Barta-Rajnai E, Jakab E, Sebestyen Z, May Z, Barta Z, Wang L and etc., Comprehensive Compositional Study of Torrefied Wood and Herbaceous Materials by Chemical Analysis and Thermoanalytical, Energy Fuels 30 (10) (2016) 8019–30.

[42] Tumuluru JS, Effect of Deep Drying and Torrefaction Temperature on Proximate, Ultimate Composition, and Heating Value of 2-mm Lodgepole Pine (*Pinus contorta*) Grind, Bioengineering 3 (16) (2016) 1–18.

[43] Turner I, Rousset P, Remond R, Perre P, An Experimental and Theoretical Investigation of the Thermal Treatment of Wood (*Fagus sylvatica L.*) in the Range 200–260°C, 3^{rd} Int Symp Energy Biomass Waste (2010) 1–2.

[44] Basu P, Rao S, Dhungana A, An investigation into the effect of biomass particle size on its torrefaction, The Can J Chem Eng 91 (3) (2013) 466–74.

[45] Encinar JM, Beltran FJ, Bernalte A, Ramiro W, Gonzalex JF, Pyrolysis of Two Agricultural Resides: Olive and Grape Bagasse. Influence of Particle Size and Temperature, Biomass Bioenergy 11 (5) (1996) 397–409.

[46] Trubetskaya A, Surup GR, Bates RB, Shapiro A, Modeling the influence of potassium content and heating rate on biomass pyrolysis, Appl Energy 194 (2017) 199–211.

[47] Cellatoglu N, Ilkan M, Torrefaction of Solid Olive Mill Residue, Bioresources 10 (3) (2015) 5876–89.

[48] Neupane S, Adhikari S, Wang Z, Ragauskas AJ, Pu Y, Effect of torrefaction on biomass structure and hydrocarbon production from fast pyrolysis, Green Chem 17 (2015) 2406–17.

[49] Shoulaifar TK, DeMartini N, Willfor S, Pranovich A, Smeds AI and etc., Impact of torrefaction on the chemical structure of birch wood, Energy Fuel 28 (2014) 3863–72.

[50] Chen L, Wang X, Yang H, Lu Q, Yang H and etc., Study on pyrolysis behaviors of non-woody lignins with TG-FTIR and Py-GC/MS, J Anal Appl Pyrolysis 113 (2015) 499–507.

[51] Fardim P, Duran N, Modification of fibre surfaces during pulping and refining as analysed by SEM, XPS and ToF-SIMS, Colloids Surf 223 (2003) 263–76.

[52] Grams J, Ruppert AM, Niewiadomski M, Jedrzejczyk M, Rzeznicka I, Surface characterization of lignocellulosic biomass submitted to pyrolysis, Surf Interface Anal 46 (2014) 837–41.

[53] Ruppert AM, Grams J, Cacciaguerra T, Swierczynski D, Investigation of biomass depolymerisation by surface techniques, Surf Interface Anal 46 (2014) 832–6.

[54] Grams J, New Trends and Potentialities of ToF-SIMS in Surface Studies, Nova Science Pulishers Inc, 2007.

[55] Strzelec K, Baczek N, Ostowska S, Wasikowska K, Szynkowska MI, Grams J, Synthesis and characterization of novel polythiourethane hardeners for epoxy resins, CR Chimie 15 (2012) 1065–71.

[56] Bielinski D, Lipinski P, Slusarski L, Grams J, Paryjczak T, Jagielski J and etc., Surface layer modification of ion bombarded HDPE, Surf Sci 564 (2004) 179–86.

[57] Brunelle A, Touboul D, Laprevote O, Biological tissue imaging with time-of-flight secondary ion mass spectrometry and cluster ion sources, J Mass Spectrom 40 (8) (2005) 985–99.

[58] Belu AM, Graham DJ, Castner DG, Time-of-flight secondary ion mass spectrometry:techniques and applications for the characterization of biomaterial surfaces, Biomat 24 (21) (2003) 3635–53.

[59] Goacher RE, Jeremic D, Master ER, Expanding the library of secondary ions that distinguish lignin and polysaccharides in time-of-flight secondary ion mass spectrometry analysis of wood, Anal Chem 83 (657) (2011) 804–12.

[60] Tolbert A, Ragauskas AJ, Advances in understanding the surface chemistry of lignocellulosic biomass via time-of-flight secondary ion mass spectrometry, Energy Sci Eng 5 (1) (2017) 5–20.

[61] Gholamzadeh N, Peyravi M, Jahanshahi M, Study on Olive Oil Wastewater Treatment: Nanotechnology Impact, J Water Environ Nanotechnol 1 (2) (2016) 145–61.

[62] Agar DA, Kwapinska M, Leahy JJ, Pyrolysis of wastewater soludge and composted organic fines from minicipal solid waste: laboratory reactor characterisation and product distribution, Env Sci Poll Research 25 (2018) 35874–82.

[63] Sangines P, Dominguez MP, Sanchez F, San Miguel G, Slow pyrolysis of olive stones in a rotary kiln: Chemical and energy characterization

of solid, gas, and condensable products, J Ren Sust Energy 7 (043103) (2015) 1–13.

[64] Surup GR, Leahy JJ, Timko MT, Trubetskaya A, Hydrothermal carbonization of olive wastes to produce renewable, binder-free pellets for use as metallurgical reducing agents, Ren Energy 155 (2020) 347–57.

[65] Serrano D, Kwapinska M, Horvat A, Sanchez-Delgado S, Leahy JJ, Cynara cardunculus L, gasification in a bubbling fluidized bed: The effect of magnesite and olivine on product gas, tar and gasification performance, Fuel 173 (2016) 247–59.

[66] Hayes DJ, Analysis of Lignocellulosic Feedstocks for Biorefineries with a Focus on the Development of Near Infrared Spectroscopy as a Primary Analytical Tool. PhD thesis, University of Limerick, 2011.

[67] Saleh SB, Torrefaction of Biomass for Power Production. PhD thesis, Technical University of Denmark, 2013.

[68] Binti Saleh S, Brun Hansen B, Jensen PA, Dam-Johansen K, Influence of Biomass Chemical Properties on Torrefaction Characteristics, Energy Fuels 27 (2013) 7541–8.

[69] Wang Z, Wang F, Cao J, Wang J, Pyrolysis of pine wood in a slowly heating fixed-bed reactor: Potassium carbonate versus calcium hydroxide as a catalyst, Fuel Process Tech 98 (8) (2010) 942–50.

[70] Romero E, Quirantes M, Nogales R, Characterization of biomass ashes produced at different temperatures from olive-oil-industry and greenhouse vegetable wastes, Fuel 208 (2017) 1–9.

[71] Sommersacher P, Kienzl N, Evic N, Hochenauer C, The Influence of Torrefaction on the Combustion Behavior of Selected Agricultural and Waste-Derived Solid Biomass Fuels, Chem Eng Trans 65 (2018) 361–6.

[72] Kung KS, Thengane SK, Shanbhogue S, Ghoniem AF, Parametric analysis of torrefaction reactor operating under oxygen-lean conditions, Energy 181 (2019) 603–14.

[73] Kung KS, Thengane SK, Ghoniem AF, Functional mapping of torrefied product characteristics with index of torrefaction, Fuel Process Tech 202 (2020) 106362.

[74] Bates RB, Ghoniem AF, Biomass torrefaction: Modeling of volatile and solid product evolution kinetics, Biores Technol 124 (2012) 460–9.

[75] Peng JH, Bi HT, Sokhansanj S, Lim JC, A Study of Particle Size Effect on Biomass Torrefaction and Densification, Energy Fuels 26 (2012) 3826–39.

[76] Shen J, Wang XS, Garcia-Perez M, Mourant D, Rhodes MJ, Li MJ and etc., Effects of particle size on the fast pyrolysis of oil mallee woody biomass, Fuel 88 (2009) 1810–7.

[77] Gaston KR, Jarvis MW, Pepiot P, Smith KM, Frederick WJ, Nimlos MR and etc., Biomass pyrolysis and gasification of varying particle sizes in a fluidized-bed reactor, Energy Fuels 25 (2011) 3747–57.

[78] Yang H, Yan R, Chen H, Lee DH, Zheng C, Characteristics of hemicellulose, cellulose and lignin pyrolysis, Fuel 86 (2007) 1781–8.

[79] Xue G, Kwapinska M, Kwapinska W, Czajka KM, Kennedy J, Leahy JJ, Impact of torrefaction in properties of *Miscanthus* x *giganteus* relevant to gasification, Fuel 121 (2014) 189–97.

[80] Basu P, Biomass Gasification and Pyrolysis: Practical Design and Theory, Elsevier, 2010.

[81] Tumuluru JS, Hess JR, Boardman RD, Wright CT, Westover TL, Formulation, Pretreatment, and Densification Options to Improve Biomass Specifications for Co-Firing High Percentages with Coal, Ind Biotech 8 (3) (2012) 113–32.

[82] Medic D, Investigation of torrefaction process parameters and characterization of torrefied biomass. PhD thesis, Iowa State University, 2012.

[83] Schwanninger M, Rodriques JC, Pereira H, Hinterstoisser B, Effects of short-time vibratory ball milling on the shape of FT-IR spectra of wood and cellulose, Vib Spectrosc 36 (2004) 23–40.

[84] Traore M, Kaal J, Cortizas AM, Application of FTIR spectroscopy to the characterization of archeological wood, Spectrochim Acta A 153 (2016) 63–70.

[85] Colom X, Carrillo F, Nogues F, Carriga P, Structural analysis of photodegraded wood by means of FTIR spectroscopy, Polym Degrad Stabil 80 (2003) 543–9.

[86] Chen H, Ferrari C, Angiuli M, Yao J, Raspi C, Bramanti E, Qualitative and quantitative analysis of wood samples by Fourier transform

infrared spectroscopy and multivariate analysis, Carbohydr Polym 82 (2010) 772–8.

[87] El-Hendawy ANA, Variation in the FTIR spectra of a biomass under impregnation, carbonization and oxidation conditions, J Anal Appl Pyrolysis 75 (2004) 159–66.

[88] Arellano O, Flores M, Guerra J, Hidalgo A, Rojas D, Strubinger A, Hydrothermal Carbonization of Corncob and Characterization of the Obtained Hydrochar, Chem Eng Trans 50 (2016) 235–40.

[89] Adapa PK, Tabil LG, Schoenau GJ, Canam T, Dumonceaux T, Quantitative Analysis of Lignocellulosic Components of Non-Treated and Steam Exploded Barley, Canola, Oat and Wheat Straw Using Fourier Transform Infrared Spectroscopy, J Agr Sci Tech B 1 (2011) 177–88.

[90] Fan M, Dai D, Huang B, Chapter 3 Fourier Transform Infrared Spectroscopy for Natural Fibres. In (ed. Salih SM): Fourier Transform, IntechOpen (2012) 45–68.

[91] Ahmad F, Silva EL, Varesche MBA, Hydrothermal processing of biomass for anaerobic digestion - A review, Renew Sust Energ Rev 98 (2018) 108–24.

[92] Sakaki T, Shibata M, Sumi T, Yasuda S, Saccharification of Cellulose Using a Hot-Compressed Water-Flow Reactor, Ind Eng Chem Res 41 (4) (2002) 661–5.

[93] Trubetskaya A, Jensen PA, Jensen AD, Glarborg P, Larsen Andresen M, Hofmann Larsen F, Characterization of free radicals by electron

spin resonance spectroscopy in biochars from pyrolysis at high heating rates and at high temperatures, Biomass Bioenergy 94 (2016) 117–29.

[94] Gai X, Wang H, Liu J, Zhai L, Liu S, Ren T and etc., Effects of Feedstock and Pyrolysis Temperature on Biochar Adsorption of Ammonium and Nitrate, PLOS one 9 (12) (2014) 1–19.

[95] Takaya CA, Parmar KR, Fletcher LA, Ross AB, Biomass-Derived Carbonaceous Adsorbents for Trapping Ammonia, agriculture 9 (1) (2019) 1–16.

[96] Grams J, Kwapinska M, Jedrzejczyk M, Rzeznicka I, Leahy JJ, Ruppert AM, Surface characterization of Miscanthus x giganteus and Willow subjected to Torrefaction, J Anal Applied Pyrolysis 138 (2019) 231–41.

[97] Saito K, Kato T, Takamori H, Kishimoto T, Yamamoto A, Fukushima K, A new analysis of the depolymerized fragments of lignin polymer in the plant cell walls using ToF-SIMS, Appl Surf Sci 252 (2006) 6734–7.

[98] Tokareva EN, Pranovich AV, Holmbom BR, Characteristic fragment ions from lignin and polysaccharides in ToF-SIMS, Wood Sci Technol 45 (2011) 767–85.

[99] Zhou C, Li Q, Chiang VL, Lucia LA, Griffis DP, Chemical and spatial differentiation of syringyl and guaiacyl lignins in poplar wood via time-of-flight secondary ion mass spectrometry, Anal Chem 83 (2011) 7020–6.

[100] Dumitrache A, Akinosho H, Rodriquez M, Meng X, Yoo CG, Natzke J and etc., Consolidated bioprocessing of Populus using Clostridium (ruminiclostridium) thermocellum: a case study on the impact of lignin composition and structure, Biotechnol Biofuels 9 (2016) 1–14.

[101] Saito K, Mitsutani T, Imai T, Matsushita Y, Yamamoto A, Fukushima K and etc., Chemical differences between sapwood and heartwood of Chamaecyparis obtuse detected by ToF-SIMS, Appl Surf Sci 255 (2008) 1088–91.

[102] Deng J, Wang GJ, Kuang JH, Zhang YL, Luo YH, Pretreatment of agricultural residues for co-gasification via torrefaction, J Anal Appl Pyrolysis 86 (2009) 331–7.

[103] Surup GR, Heidelmann M, Schubert D, Deike R, Foppe M, Trubetskaya A and etc., The effect of feedstock origin and temperature on the structure and reactivity of char from pyrolysis at 1300-2800°C, Fuel 235 (2019) 306–16.

[104] Binti Saleh S, Brun Hansen B, Jensen PA, Dam-Johansen K, Demartini N, Egsgaard H and etc., Release of Chlorine and Sulfur during Biomass Torrefaction and Pyrolysis, Energy Fuels 28 (6) (2014) 3738–46.

[105] Ramesh MN, Effect of cooking and drying on the thermal conductivity of rice, Int J Food Prop 3 (1) (2000) 77–92.

[106] Guo W, Lim JC, Bi XT, Sokhansanj S, Melin S, Determination of effective thermal conductivity and specific heat capacity of wood pellets, Fuel 103 (2013) 347–55.

[107] Mason PE, Darvell LI, Jones JM, Williams A, Comparative Study of the Thermal Conductivity of Solid Biomass Fuels, Energy Fuels 30 (2016) 2158–63.

[108] Hobani AI, Tolba MH, Bulk Thermal Conductivity and Diffusivity of Barley, Res Bult 53 (1995) 5–17.

[109] Hlosta J, Zurovec D, Gelnar D, Zegzulka J, Thermal Conductivity Measurement of Bulk Solids, Chem Eng Tech 40 (10) (2017) 1876–84.

[110] Blomqvist P, Sjöström J, Direct measurements of thermal properties of wood pellets: Elevated temperatures, fine fractions and moisture content, Fuel 134 (2014) 460–6.

[111] Xu Z, Zinchik S, Kolapkar SS, Bar-Ziv E, Hansen T, Conn D and etc., Properties of Torrefied U.S. Waste Blends, Front Energy Res 8 (65) (2018) 1–13.

[112] Surup GR, Heidelmann M, Kofoed Nielsen H, Trubetskaya A, Characterization and reactivity of charcoal from high temperature pyrolysis (800-1600°C), Fuel 235 (2019) 1544–54.

[113] Sluiter A, Hames B, Ruiz R, Scarlata C, Sluiter J, Templeton D et al., Determination of Structural Carbohydrates and Lignin in Biomass. Golden (CO): National Renewable Energy Laboratory; Report No. NREL/TP-510-42618. Contract No.: DE-AC36-08-GO28308 .

[114] Willför S, Hemming J, Leppänen AS, Analysis of extractives in different pulps - Method development, evaluation, and recommendations.

Finland: Åbo Akademi University, Laboratory of Wood and Paper Chemistry; Report No. B1 of the EU COST E41 action "Analytical tools with applications for wood and pulping chemistry" .

[115] Hames B, Ruiz R, Scarlata C, Sluiter J, Sluiter A, Preparation of Samples for Compositional Analysis. Golden (CO): National Renewable Energy Laboratory; Report No. NREL/TP-510-42620. Contract No.: DE-AC36-99-GO10337 .

[116] Thammasouk K, Tandjo D, Penner MH, Influence of Extractives on the Analysis of Herbaceous Biomass, J Agric Food Chem 45 (1997) 437–43.

[117] Kers J, Kulu P, Aruniit A, Laurmaa V, Krizan P, Soos L and etc., Determination of physical, mechanical and burning characteristics of polymeric waste material briquettes, Estonian J Eng 16 (4) (2010) 307–16.

[118] Tanui JK, Kioni PN, Kariuki PN, Ngugi JM, Influence of processing conditions on the quality of briquettes produced by recycling charcoal dust, Int J Energy Env Eng 9 (3) (2018) 341–50.

[119] Liu X, Bi XT, Removal of inorganic consituents from pine barks and switchgrass, Fuel Process Tech 92 (7) (2011) 1273–9.

[120] Trubetskaya A, Jensen PA, Jensen AD, Steibel M, Spliethoff H, Glarborg P and etc., Comparison of high temperature chars of wheat straw and rice husk with respect to chemistry, morphology and reactivity, Biomass Bioenergy 86 (2016) 76–87.

[121] Rodriquez G, Lama A, Rodriquez R, Jimenez A, Guillen R, Fernandez-Bolanos J, Olive stone an attractive source of bioactive and valuable compounds, Biores Tech 99 (2008) 5261–9.

[122] Kim YH, Na BI, Ahn B, Lee HW, Lee JW, Optimal condition of torrefaction of high energy density solid fuel of fast growing tree species, Korean J Chem Eng 32 (8) (2015) 1547–53.

[123] Bastakoti N, Dhital HC, Aryal A, Study of effects of temperature and residence time on calorific value of torrefied biomass, Int J Eng Tech 7 (10) (2019) 31–5.

- Temperature and residence time strongly affect CO_2 reactivities of torrefied material
- Small olive stones contain more cellulose and lignin than large particles
- Large particle size and high moisture content in biomass decrease the thermal conductivity
- Calorific values of torrefied olive stones were below the values of peat and coal

Letter of interest for the manuscript "The effect of particle size, temperature and residence time on the yields and reactivity of olive stones from torrefaction"

Dear editor,

We as authors declare that we have no known competing financial interests or personal relationships that could have appeared to influence the work reported in this paper.

Best Regards,

Anna Trubetskaya, James J Leahy, Marzena Kwapinska, Jacek Grams and Robert Johnson